Available online at www.sciencedirect.com

ScienceDirect

Geochimica et Cosmochimica Acta 321 (2022) 133–154

Geochimica et Cosmochimica Acta

www.elsevier.com/locate/gca

Source to sink analysis of weathering fluxes in Lake Baikal and its watershed based on riverine fluxes, elemental lake budgets, REE patterns, and radiogenic (Nd, Sr) and $^{10}Be/^{9}Be$ isotopes

Tim Jesper Suhrhoff [a,*], Jörg Rickli [a], Marcus Christl [b], Elena G. Vologina [c], Viet Pham [d], Moustafa Belhadj [d], Eugene V. Sklyarov [c], Catherine Jeandel [d], Derek Vance [a]

[a] *ETH Zürich, Institute of Geochemistry and Petrology, Department of Earth Sciences, Clausiusstrasse 25, 8092 Zürich, Switzerland*
[b] *ETH Zurich, Laboratory of Ion Beam Physics, Schafmattstr. 20, HPK G23, CH-8093 Zurich, Switzerland*
[c] *Institute of the Earth's Crust, Siberian Branch of the RAS, Irkutsk 664033, Russia*
[d] *Laboratoire d'Etudes en Géophysique et Océanographie Spatiale (LEGOS, Université de Toulouse, CNRS, CNES, IRD, UPS), 31400 Toulouse, France*

Received 27 June 2021; accepted in revised form 8 January 2022; available online 15 January 2022

Abstract

We present a detailed analysis of weathering fluxes at Lake Baikal, the largest lake in the world, using the major element, trace element and isotope geochemistry of major inflowing rivers, the lake itself, and its sediments. Our objective is to assess how lake records could be used to understand river-catchment-scale denudation and weathering processes.

Total denudation rates at Lake Baikal, as obtained from meteoric $^{10}Be/^{9}Be$, are an order of magnitude lower than the global average, at 16–35 t km^{-2} yr^{-1}. Chemical weathering rates obtained from the riverine dissolved load and discharge are, on the other hand, in the same range as global values, at 6–29 t km^{-2} yr^{-1}. Chemical weathering rates are higher in the north of the catchment than in the south, consistent with higher runoff in the north. In contrast, $^{10}Be/^{9}Be$-derived denudation rates are higher in the south. We hypothesize that this pattern of variation may be due to the stabilizing effect of permafrost soils preventing erosion in the north. An inverse model shows that the Selenga River, Lake Baikal's major tributary, has a silicate weathering contribution to riverine dissolved cation fluxes of 42 mol%; this and other characteristics are representative of large rivers globally. Many trace elements have much lower concentrations in the lake than in inflowing rivers (Be (5%), Mn (3%), Fe (0.4%) and REE (1–2%)). We suggest, based on REE patterns and Mn, Fe-depth profiles in the lake, that this removal is the result of pH induced changes in dissolved-adsorbed partitioning at the river-lake interface, and the incorporation of trace elements into authigenic Fe-Mn (oxyhydr)oxide phases forming within the lake. Strontium is isotopically uniform within the lake, demonstrating that the whole lake mixes on a timescale shorter than its residence time (<330 years). Neodymium and Be, in contrast, show isotopic variability between the basins. While the Sr isotope budget of the lake is largely consistent with observed riverine Sr fluxes, an unradiogenic Nd source is needed to explain lake Nd isotope compositions, especially in the Northern Basin. This source appears to derive from old crustal rocks in this part of the catchment and could be hydrothermal, or small rivers that were not sampled here. Similarly, elevated $^{10}Be/^{9}Be$ ratios in the lake basins relative to the river input imply variable but significant atmospheric inputs of ^{10}Be into the lake.

* Corresponding author.
E-mail address: tjsuhrhoff@erdw.ethz.ch (T.J. Suhrhoff).

https://doi.org/10.1016/j.gca.2022.01.007
0016-7037/© 2022 The Authors. Published by Elsevier Ltd.
This is an open access article under the CC BY license (http://creativecommons.org/licenses/by/4.0/).

Overall, this study demonstrates that records of the paleo-chemistry of lakes, and Lake Baikal in particular, hold promise for understanding denudation and weathering on the continents, in ways that are more directly relatable to the environmental conditions of the catchment than is possible with marine records.
© 2022 The Authors. Published by Elsevier Ltd. This is an open access article under the CC BY license (http://creativecommons.org/licenses/by/4.0/).

Keywords: Lake Baikal; Weathering; Erosion; Denudation; Meteoric beryllium; Radiogenic isotopes; REE

1. INTRODUCTION

The chemical weathering of continental rocks is a key surface Earth process that controls pedogenesis, the chemical composition of rivers, and the transfer of dissolved elements to the oceans, where it represents a significant source term for the oceanic biogeochemical cycles of many elements. Methods used to study modern chemical weathering fluxes are mainly based on the chemical composition of rivers, utilizing major ion composition and runoff to calculate chemical weathering fluxes directly (e.g. Gaillardet et al., 1999; Viers et al., 2013). In addition, a large variety of isotope systems offer insight into weathering and denudation rates (e.g., meteoric $^{10}Be/^{9}Be$ ratios or in-situ cosmogenic ^{10}Be and ^{26}Al, e.g. von Blanckenburg, 2005; von Blanckenburg et al., 2012), sources of weathering fluxes (e.g., radiogenic Sr and Nd isotopes; e.g. Blum and Erel, 2003), or weathering intensity (e.g., Li isotopes; Dellinger et al., 2015).

Records of climate and weathering rates in the past are central to our understanding of this important carbon cycle process. Studies of *continental* paleo-weathering rates are usually based on *marine* sediment cores. But it is often inherently difficult to relate continental weathering processes to marine sediment cores due to the different spatial scales of the processes involved. Authigenic marine sedimentary phases reflect weathering signals on global (Sr), on ocean basin (Nd, Be), or on more local scales (Pb) depending on the elements' marine residence time. As a result, interpreting the scale gap between riverine chemical signatures, with different responses to regionally-variable parameters such as climate, and what is recorded in a marine sediment can be difficult.

Here, we explore how lakes could be used to more directly assess how river-catchment-scale denudation and weathering processes are reflected in sedimentary records. Due to their large catchment areas, the water chemistry of large lakes integrates chemical weathering processes over significant portions of the Earth's surface. At the same time, catchments can be small enough to exhibit a spatially uniform response to environmental change. The intermediate scale also means that the chemical weathering budgets of lakes and their catchments are easier to study and quantify compared to ocean basins. The very long residence times of some elements in the oceans, such as Sr, means that they do not respond to changes in inputs driven by short- to medium-term climate change, a difficulty that can also potentially be overcome through lake studies. Thus, lake archives may help to understand spatial and temporal patterns in chemical weathering resulting from changing climate conditions.

To explore this potential, we investigate weathering and denudation across the catchment of the most voluminous lake in the world - Lake Baikal. We first assess denudation, chemical weathering, and physical erosion fluxes in the major riverine sources to Lake Baikal. Specifically, we use major element concentrations and their ratios, in combination with an inverse model, to assess whether Lake Baikal is a suitable location to study the weathering of silicate rocks. Further, we utilize published suspended matter fluxes (Potemkina, 2011) and meteoric Be isotopes to calculate denudation fluxes (von Blanckenburg et al., 2012), and Sr and Nd isotopes as tracers of weathering sources (e.g. Blum and Erel, 2003). Second, we evaluate how riverine fluxes are transferred into the lake by studying how the concentrations of a large array of elements, including rare earth elements (REE), differ between the rivers and the lake. Third, we assess how well mixed the lake is with regard to dissolved Be, Nd, and Sr isotope compositions, which is important in identifying the processes governing variability in sediment cores. The integrated observations, linking river and lake chemistry, provide a robust modern framework for the study of past weathering conditions at Lake Baikal.

2. SETTING AND METHODS

2.1. Lake Baikal

Lake Baikal contains about 20% of all non-frozen freshwater on Earth (Sherstyankin et al., 2006). The lake is subdivided into a Northern, a Central, and a Southern Basin by the Academician Ridge in the north, and the Buguldeika Ridge, with its overlying Selenga delta sediments, in the south (Fig. 1). The water column remains stratified throughout the year and there is no convective overturn that is typical of many lakes. Instead, a variety of processes such as thermobaric instability (e.g. Shimaraev et al., 1993; Ambrosetti et al., 2003), thermobaric effects in combination with wind-induced and salinity driven convection (Weiss et al., 1991; Killworth et al., 1996; Hohmann et al., 1997) cause renewal of deep water at Lake Baikal. As a result, the time period over which water below 250 m depth is out of contact with the atmosphere is 8 to 18 years (Falkner et al., 1991; Weiss et al., 1991; Hohmann et al., 1997; Peeters et al., 1997). The water column is oxic throughout the whole lake (>6 mg/L O_2; e.g. Shimaraev, 1994; Martin et al., 1998).

The regional climate is continental, with very cold winters (average monthly temperatures of −12 to −19 °C) and mild summers (8 to 14 °C: Seal and Shanks, 1998). Most rain falls in summer, focusing 70–85% of the annual

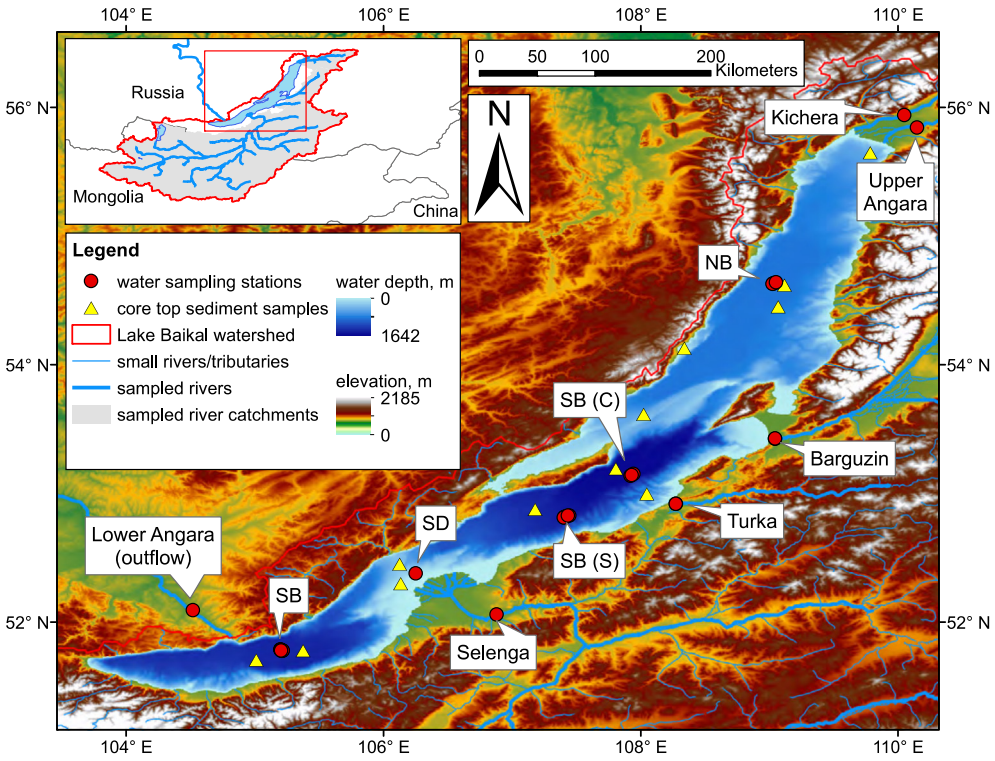


Fig. 1. Map of Lake Baikal, showing river sampling locations, stations in the lake, and the locations of analyzed core top sediments.

riverine discharge between May and September (Seal and Shanks, 1998). Riverine discharge supplies 82% of the water to the lake, precipitation 13%, and ground water discharge 5% (Colman, 1998). Most water (79%) flows out of Lake Baikal through the Angara River, with 19% lost through evaporation, and less than 2% through ground water flow (Shimaraev, 1994; Seal and Shanks, 1998). The water in the lake is replenished by river inflow in about 400 yrs (Colman, 1998). If groundwater flux, precipitation, and evaporation are included, the water residence time corresponds to 377 yrs (Colman, 1998). The residence times of most major ions in the lake are estimated to be 290–360 yrs, the exception being Cl^- at 120–140 yrs (Falkner et al., 1997). Although more than 350 rivers supply a total of 57.8 km^3 water annually (Falkner et al., 1997; Colman, 1998), four of the rivers sampled and analyzed here represent ~ 73% of this discharge: Selenga (49.3%), Upper Angara (13.7%), Barguzin (6.5%), and Turka (2.6%) (Afanasjev, 1976; Leibovich-Granina, 1987; as cited in Seal and Shanks, 1998). The Kichera River is a small tributary. There is, to our knowledge, no reliable estimate of its annual water discharge.

The catchment of Lake Baikal has several advantages for our purposes in this paper. First, the large size of the lake and its catchment (0.54 million km^2; e.g. Shimaraev, 1994) means that weathering processes can be studied on a significant spatial scale. Second, the geology of the catchment is dominated by granitoid rocks (Fagel et al., 2007), making it representative of the bulk composition of the silicate portion of the continental crust. Granitoid rocks make up 57% of surface outcrops in the Selenga and Upper Angara catchments, and 52% in the Barguzin catchment (Fagel et al., 2007). Moreover, these silicate rocks have very different ages, such that they are likely to have developed distinctive isotope signatures that could facilitate the identification of weathering signals in the lake. Archean and Proterozoic rocks dominate the watersheds of the Upper Angara, whereas the Selenga watershed is dominated by rocks of Paleozoic age (Parfenov et al., 2003; Fagel et al., 2007). In the Selenga watershed, the second most important source rocks are volcanoclastic rocks (16%), whereas in the Upper Angara watershed they are Precambrian metamorphic rocks (24%, Selenga 7%; Fagel et al., 2007). The Barguzin river watershed is dominated by Paleozoic granitoids with minor occurrences of Late Precambrian rocks (Petrov et al., 2007). On average, carbonate rocks make up less than 3% of Siberian granite units (Kulish, 1983; Yanshin, 1989, as cited in Zakharova et al., 2005). Early Paleozoic carbonates occur in the headwaters of the Selenga and, in particular, in its tributary Itanza (Petrov et al., 2007). Some small outcrops of Early Paleozoic carbonates occur in the Barguzin and Upper Angara, and Late Precambrian carbonates in the Kichera watersheds (Petrov et al., 2007). No carbonates have been reported within the Turka watershed (Petrov et al., 2007).

The catchment of Lake Baikal is characterized by significant climatic gradients. Precipitation is generally low in the southern, Mongolian, part of the catchment (less than 300 mm $year^{-1}$) and increases towards the north (400–1200 mm $year^{-1}$; Goldberg et al., 2010; Tulokhonov et al., 2015). As a result, net precipitation is only ~ 80 mm/yr in the Selenga river catchment,

but ~ 300 mm yr^{-1} in the northeastern regions of the lake, including in the Upper Angara, Kichera, and Barguzin river catchments (Afanasjev, 1976; Galazy, 1993; Shimaraev, 1994; as cited in Goldberg et al., 2010). Although also affected by altitude, air temperature generally decreases from south to north (Tulokhonov et al., 2015), accompanied by generally increasing permafrost occurrence (areal coverage) and thickness (Zakharova et al., 2005). Permafrost is also more continuous and thicker at higher altitudes (Williams and Warren, 1999; Tulokhonov et al., 2015). As a result, large parts of the Selenga river catchment have only rare islands of permafrost. The northern areas of the lake's catchment were periodically glaciated during the Quaternary (Karabanov et al., 1998; Karabanov et al., 2004). Various lines of evidence suggest at least 3–4 major glaciations at Lake Baikal (e.g. Mats, 1993), during which glaciers in the northern part extended all the way to the lake (e.g. Karabanov et al., 1998).

2.2. Analytical

Field work was conducted in August 2018 during the high discharge season. The sampling strategy was designed to assess dissolved elemental riverine fluxes, as well as the dissolved elemental budgets in the lake. Hence, 5 major tributaries were sampled, as well as 1–2 depth profiles in each of the basins (Fig. 1). Although suspended sediments and bedload were also collected for the rivers, this study focusses on the water samples. Furthermore, detrital silicate fractions of core top sediments were analyzed to constrain the isotope composition of lithologies surrounding the different basins.

Many of the analytical approaches employed here have been described previously, with the relevant work cited below. They are also presented in detail in supplement S1, which also contains more information on the analyzed sediment cores. Results are presented in Tables 1–3, including details on associated uncertainties in the footnotes (see also Section 2.3).

In brief, water samples were filtered in the field (0.45 µm Supor filter) and acidified to pH < 2. Cations, except Be and REE, were measured without pre-concentration on a Thermo Finnigan Element XR (in Zurich; Vance et al., 2016). The precision ranged from 2-7% (unless specified otherwise, all uncertainties in this study correspond to 2SD). For most elements, accuracy was within 5–15% with the exception of P, Mo, and Pb (within 25% of the certified values). Concentrations were adjusted to certified or literature values of SLRS 6 (Yeghicheyan et al., 2019). Be was preconcentrated prior to measurement by evaporating larger sample volumes. Duplicate measurements yield uncertainty estimates of 2.6% for the river samples and 4% for the lake (Suhrhoff et al., 2019). REE were preconcentrated on NOBIAS-chelate PA-1® resin using a manifold system inspired by Biller and Bruland (2012) and Hatje et al. (2014) and measured on a Thermo Finnigan Element 2 (in Toulouse) using a combination of isotope dilution (with a triple spike of Nd, Eu, and Yb) and external calibrations (Pham et al., 2019). Average procedural blanks were < 1% of sample REE content, except for Ce (<3%) in some deep lake samples (>250 m). External uncertainties estimated from 7 full seawater replicates corresponds to < 1.1% for all REE, except Yb (1.7%) and Nd (1.2%). The river and lake samples were run at lower concentrations with an average internal uncertainty of 4.8% and a range between 1.7 and 9.8%. Internal uncertainties are shown in Fig. 4 and supplement S4. Anions were measured by ion chromatography on a Thermo Dionex IonPac AS-15 column in Zurich with a precision of 3 to 3.5%.

The measurement of Nd and ^{10}Be isotopes in river and lake waters required pre-concentration by Fe-coprecipitation from large volumes of filtered water (12.7 to 19.3 L). Iron was subsequently separated on anion resin (AGMP1), prior to the separation of Be, Sr and REE on cation resin (AG 50 W-X8). Sr and Nd were further purified on Sr Spec and LN Spec resins (Pin and Zalduegui, 1997; Deniel and Pin, 2001). ^{10}Be concentrations were measured on the ETH Zurich AMS facility Tandy (Müller et al., 2010; Christl et al., 2013) after addition of 300 µg ^{9}Be carrier. Resulting uncertainties for the natural $^{10}Be/^{9}Be$ ratios are 5.6–7.5% for river samples, and 7.8–11.2% for lake samples.

Detrital silicate phases of sediments, measured for Sr and Nd isotopes, were dissolved after sequential leaching and removal of FeMn-oxides and opal (Olivarez Lyle and Lyle, 2002; Wiederhold et al., 2007). Sr and Nd were separated and further purified as detailed for the water samples, although without an initial anion column.

Sr and Nd isotopes of water samples and sediments were measured on a Thermo Fisher Neptune MC-ICP-MS and internally normalized for instrumental mass bias following Thirlwall (1991) for Sr and Vance and Thirlwall (2002) for Nd. Sample Sr and Nd isotope compositions were renormalized to the accepted literature values of the run standard solutions (NIST SRM 987 and La Jolla standards respectively; Thirlwall, 1991). These session-specific corrections were < 38 ppm for Sr and < 11 ppm for Nd. External uncertainty estimates of the isotope measurements based on repeated standard measurements (n > 12) correspond to 12 ppm for $^{87}Sr/^{86}Sr$ and 15 to 22 ppm for ε_{Nd}, depending on sample concentration at measurement. Repeat measurements of USGS reference material Nod A-1, processed with the samples, yielded $^{143}Nd/^{144}Nd = 0.512150 \pm 6$ (n = 9) and $^{87}Sr/^{86}Sr = 0.709197 \pm 9$ (n = 6), consistent with the literature (Foster and Vance, 2006).

Procedural blanks for isotope measurements include the handling and reagent blanks from the field as well as subsequent processing in the clean lab. Two full procedural blanks, including the blanks of all chemicals and the laboratory procedure, were obtained. The procedural blank of Sr corresponds to less than 0.05% of sample Sr. Nd blank contributions are < 0.6% for rivers and lake samples shallower than 500 m. For deeper samples, maximal blank contributions correspond to 2.5%. No blank corrections were applied for Sr and Nd isotopes. For ^{10}Be, the average procedural blank corresponds to ~ 0.5% of average sample ^{10}Be, with a maximum of ~ 3.3%. As the ^{10}Be blank could not be quantified precisely, no corrections were applied to the samples.

Table 1
Physico-chemical parameters, catchment properties, and meteoric ^{10}Be fluxes for the rivers analyzed in this study.

	Sampling location		*I. physico-chemical parameters*				*II. catchment properties*				
River Unit	LON °	LAT °	T °C	pH	Conductivity µS cm^{-1}	Alkalinity mg L^{-1} as CaCO3	Slope [b] °	Area [b] km^2	Discharge [c] km^3 yr^{-1}	Runoff [d] mm yr^{-1}	$F^{^{10}Be}_{met}$ t km^{-2} yr^{-1}, *10^{-13}
Selenga	106.879343	52.05789	21.1	7.82	144.9	57	1.12	450,065	28.5	63	2.29 ± 0.35 [e]
Turka	108.274321	52.917765	18.8	8.32	64.7	26.8	1.47	5947	1.48	249	1.79 ± 0.18 [e]
Barguzin	109.044596	53.423251	21	7.5	169	70.6	1.86	21,176	3.75	177	1.52 ± 0.15 [e]
Upper Angara	110.148187	55.844173	14.4	7.81	118.2	48.8	2.35	20,786	7.91	380	1.35 ± 0.07 [e]
Kichera	110.048862	55.940959	13	6.84	46.5	16.6	2.98	1336	-	-	1.39 ± 0.07 [e]
2SD ext. uncertainty	-	-	0.1[a]	0.05[a]	2 %[a]	1.1[a]	-	-	-	-	-

a) Based on replicate measurements of lake water.
b) Based on GIS analysis in ArcMap.
c) Compiled from Falkner et al., (1997) and Colman (1998).
d) Calculated from river discharge (Falkner et al., 1997; Colman, 1998) and catchment area.
e) Uncertainty deduced from the variability in flux estimates within each riverine catchment (1SD; Heikkilä and Smith, 2013; Heikkilä et al., 2013; Heikkilä and von Blanckenburg, 2015). For the small Kichera catchment, which is contained within one cell of the atmospheric ^{10}Be flux map, we use the uncertainty of the adjacent Upper Angara catchment.

2.3. Denudation, erosion, and weathering parameters

Here, we refer to denudation rate (D_{E+W}) as the sum of catchment area-normalized *chemical* weathering (W) and *physical* erosion rates (E) expressed in tons (t, solid or dissolved elements) km^{-2} yr^{-1}.

$$D_{E+W} = E + W \tag{1}$$

Physical erosion rates (E) were calculated from detailed time series of sediment fluxes for the Selenga, Barguzin and Upper Angara rivers ($J_{sediment}$, converted to t yr^{-1}; Potemkina, 2011) and the surface area of the catchment (A, in km^2, extracted using ArcGIS):

$$E = \frac{J_{sediment}}{A} \tag{2}$$

Although these time series span multiple decades, we only use the last decade of available data (i.e. 1995 to 2005, $E_{1995\text{-}2005}$) because agricultural activity temporarily increased erosion rates above natural levels up until about 1980 (Chalov et al., 2014). The most recent data for the Selenga River is compatible with other high frequency observations from 2011 (Chalov et al., 2014).

Chemical weathering rates (W) were calculated from Q, A, and observed total dissolved solid (TDS, converted to t km^{-3}) concentrations after subtracting atmosphere-derived bicarbonate ($HCO^-_{3,atm}$, converted to t km^{-3}):

$$W = \frac{Q * \left(TDS - HCO^-_{3,atm}\right) * SV}{A} \tag{3}$$

where TDS is the sum of all cations and anions, HCO^-_{3atm} is calculated from the results of an inverse model (Section 4.1), and SV accounts for seasonal variation (1.1 ± 0.1, 1 SD). Correction for the impact of seasonal variation, i.e. dilution in the high discharge season (Berner and Berner, 2012; Milliman and Farnsworth, 2013), and its uncertainty were estimated using seasonal major cation data of two Siberian rivers (600 km distance from Lake Baikal; Zakharova et al., 2005). Uncertainties on D_{E+W}, E and W were estimated by propagating uncertainties of all relevant parameters in Eqs. (1)–(3).

Additionally, assuming that dissolved ^{10}Be/^{9}Be ratios have isotopically equilibrated with reactive Be adsorbed to particle surfaces and bound in Fe-oxyhdroxides (von Blanckenburg et al., 2012), riverine denudation rates were also deduced from dissolved ^{10}Be/^{9}Be ratios (D_{Be}; von Blanckenburg et al., 2012):

$$D_{Be} = \frac{F^{^{10}Be}_{met}}{\left(\frac{^{10}Be}{^{9}Be}\right)_{diss} * [^9Be]_{parent} * \left(f^{^{9}Be}_{reac} + f^{^{9}Be}_{diss}\right)} \tag{4}$$

where $F^{^{10}Be}_{met}$ is the meteoric flux of ^{10}Be (converted to t km^{-2} yr^{-1}, see Table 1), calculated for each catchment from a map of modelled modern meteoric ^{10}Be fluxes (Heikkilä and Smith, 2013; Heikkilä et al., 2013; Heikkilä and von Blanckenburg, 2015), $\left(\frac{^{10}Be}{^{9}Be}\right)_{diss}$ is the ratio of ^{10}Be/^{9}Be isotopes measured in the riverine dissolved phases, $[^9Be]_{parent}$ is the concentration of Be in rocks undergoing weathering (in ppm), and $\left(f^{^{9}Be}_{reac} + f^{^{9}Be}_{diss}\right)$ refers to the mobile fraction

Table 2
Isotope compositions and weathering parameters for the rivers analyzed in this study. Given uncertainties correspond to 2 SD for all isotope compositions and TDS, and to 1 SD for weathering, erosion and denudation rates. Details on the uncertainty estimates are given in the footnotes and in Sections 2.2 and 2.3.

River	*I. isotope composition*			*II. TDS, weathering, erosion, and denudation*					
	$^{10}Be/^{9}Be$ [a]	ε_{Nd} [b]	$^{87}Sr/^{86}Sr$ [b]	TDS [e]	W [f]	E		D	
						$E_{1995\text{-}2005}$ [g]	$E_{this\ study}$ [h]	D_{E+W} [j]	D_{Be} [j]
Unit	$*10^{-8}$			mg L^{-1}	t km^{-2} yr^{-1}	t km^{-2} yr^{-1}	t km^{-2} yr^{-1}	t km^{-2} yr^{-}	t km^{-2} yr^{-1}
Selenga	0.82 ± 0.05	−5.02 ± 0.08	0.708103 ± 11	119.8 ± 9.2	5.7 ± 0.9	2.2 ± 0.1	2.6 ± 0.2	7.9 ± 0.9	34.7 ± 11.5
Turka	0.76 ± 0.04	−9.09 ± 0.07	0.708841 ± 10	65.7 ± 6.6	12.6 ± 1.8	-	0.7 ± 0.1	-	29.0 ± 9.0
Barguzin	1.07 ± 0.06	−10.92 ± 0.10	0.708484 ± 10	136.8 ± 9.5	18.9 ± 3.4	1.0 ± 0.1	1.4 ± 0.1	20.0 ± 3.4	17.5 ± 5.4
Upper Angara	1.06 ± 0.08	−8.82 ± 0.08	0.708043 ± 11	102.0 ± 7.0	29.4 ± 4.5	4.2 ± 0.2	1.3 ± 0.1	33.6 ± 4.5	15.5 ± 4.5
Kichera	0.73 ± 0.04	−10.14 ± 0.08	0.710171 ± 11	44.2 ± 3.8	-	-	-	-	23.5 ± 6.9
2SD ext. uncertainty	-	0.15–0.22[c]	0.000009[d]	-	-	-	8% [i]	-	-

a) Resulting uncertainty based on internal uncertainties of ^{10}Be measurement and the external uncertainty of repeated measurements of Be doped SLRS-6 (0.98 ppb Be).
b) Internal sample uncertainties based on internal standard error of the mean deduced from analysis on Thermo Fischer Neptune Plus.
c) Based on replicate measurements of LaJolla standard run at 15–50 ppb.
d) Based on replicate measurements of NIST 987 standard run at 100 ppb.
e) Uncertainty estimate based on the propagation of external uncertainties of individual chemical measurements.
f) Uncertainty estimate includes propagated uncertainties of all relevant parameters, using discharge time series to estimate uncertainties on riverine discharges (1 SEM on annual mean; Potemkina, 2011). For the Turka River, not available in Potemkina (2011), the maximum discharge uncertainty of other rivers was used. Corrections for atmosphere derived HCO_3^- are based on the inversion and its associated uncertainty (see Section 4.1, Table 4).
g) Uncertainty estimate based on the standard error of the mean of the time series data (1 SEM; Potemkina, 2011).
h) Estimated from suspended matter concentrations ($c_{susp,}$ in t km^{-3}, supplement S1), the annual riverine water discharge (Q in km^3; compiled from Falkner et al., 1997; Colman, 1998; Seal and Shanks, 1998), and the surface area of the catchment (A, in km^2, Table 1). As this estimate is based on a single measurement, it may not be representative of long-term erosion rates (see Sections 2.3 and 3.1). Uncertainties include propagated uncertainties of all relevant parameters.
i) Based on the uncertainty of suspended matter concentrations comparing different sample aliquot measurements.
j) Uncertainties include propagated uncertainties of all relevant parameters. See Section 2.3 for more details.

Table 3
Nd and Sr isotope composition of the detrital fractions of lake core top sediments (±internal measurement uncertainty, 2 SEM). Sample locations are sorted from north to south. NB = Northern Basin, CB = Central Basin, SB = Southern Basin.

Sample	LON, °	LAT, °	ε_{Nd}	$^{87}Sr/^{86}Sr$	Location
13–19A	109.78269	55.64939	−6.89 ± 0.08	0.708781 ± 8	North edge NB close to Upper Angara
14–8	109.11612	54.61957	−12.54 ± 0.09	0.717690 ± 9	Center of NB
14–6	109.0672	54.45098	−12.16 ± 0.09	0.714748 ± 10	Center of NB
10–12	108.33848	54.1288	–23.56 ± 0.09	0.770229 ± 9	West coast of NB
10–8/1	108.02194	53.615	−13.46 ± 0.09	0.716442 ± 9	Academician Ridge (between NB & CB)
14–9	107.80582	53.19308	−7.30 ± 0.09	0.709337 ± 10	Center of CB close to statin CB(C)
11–9	108.04603	52.99607	−8.99 ± 0.09	0.711217 ± 9	Eastern slope of CB close to Turka
10–20	107.17822	52.87622	−7.59 ± 0.07	0.710032 ± 9	Southwestern part of CB, close to station CB(S)
13–11A	106.12556	52.45	−7.31 ± 0.08	0.710151 ± 11	Buguldeika ridge (between CB &SB)
13–20b	106.13389	52.29939	−5.17 ± 0.07	0.708140 ± 10	Buguldeika ridge, closer to Selenga delta
14–3	105.37457	51.77765	−9.07 ± 0.09	0.711760 ± 11	Center of SB, east of station SB
14–2	105.0103	51.70523	−9.39 ± 0.07	0.712103 ± 9	Center of SB, west of station SB

of Be that is released from minerals during weathering and transported in the dissolved or reactive phases, i.e. adsorbed to particles or bound in secondary minerals. Due to the large scale of the Lake Baikal system and the lithologies it contains, we use the global average Be concentration of the upper continental crust of 2.5 (±0.5) ppm. For the mobile fraction, we adopt values between 0.2 to 0.5 (von Blanckenburg et al., 2012; von Blanckenburg and Bouchez, 2014; Wittmann et al., 2015; Rahaman et al., 2017), assigning them a uniform probability. The final D_{Be} and their uncertainties are based on Monte Carlo simulations (10000 runs), using parameter ranges as detailed here and the analytical uncertainty of $^{10}Be/^{9}Be$ ratios.

3. RESULTS

3.1. River data

Physico-chemical parameters, characteristic catchment properties, isotope compositions, and the calculated denudation parameters of the sampled river catchments are presented in Table 1 and Table 2. Elemental concentrations and isotope compositions are presented in supplement S4 along with measured concentrations and isotope compositions of reference materials (SLRS-6 and Nod-A). The collective riverine inputs to the lake are estimated based on river discharge weighted elemental concentrations ("rivers dw" in figure captions) and riverine elemental flux weighted isotope compositions ("rivers efw"). Results of duplicate water sample measurements are presented in supplement S1.

Of all the inflowing rivers, conductivity and alkalinity as well as major cation concentrations and TDS (Table 1 and Table 2; supplement S4), are highest in the Selenga and Barguzin rivers. The lowest concentrations are found in the Kichera River. Discharge weighted riverine conductivity and alkalinity are higher than average lake values (Fig. 2). The Selenga has the highest Nd and the second highest Sr concentration (Fig. 3), but the lowest Fe. At 28 µM, Cl concentrations are a factor of > 3 higher in the Turka River than in the other rivers.

The rivers form two groups of similar $^{10}Be/^{9}Be$ ratios (Fig. 3, Table 2). The Selenga, Turka, and Kichera Rivers yield $^{10}Be/^{9}Be$ ratios ranging from 7.3 (±0.4) – 8.2 (±0.5) × 10^{-9}. The Barguzin and Upper Angara rivers both have a somewhat higher $^{10}Be/^{9}Be$ ratio of 1.1 (±0.1) × 10^{-8}. The Selenga has the most radiogenic Nd isotope signature (ε_{Nd} of −5.2 ± 0.2), and together with the Upper Angara the least radiogenic Sr ($^{87}Sr/^{86}Sr$ of 0.708103 and 0.708043 ± 11). The most radiogenic Sr isotope signature is found in the Kichera River ($^{87}Sr/^{86}Sr$ of 0.71017 ± 11). Riverine Sr isotope compositions reported here are similar to previously reported values (Falkner et al., 1997).

Calculated chemical weathering rates W (Eq. (3), Table 2) range from 5.7 (±0.9, 1SD) t km^{-2} yr^{-1} in the Selenga to 29.4 (±4.5, 1SD) t km^{-2} yr^{-1} in the Upper Angara catchment. Sediment flux timeseries yield erosion rates of 1.0, 2.2. and 4.2 t km^{-2} yr^{-1}, for the Barguzin, the Selenga and the Upper Angara, respectively (Eq. (2); Potemkina, 2011; Chalov et al., 2014). In the Turka, E inferred from water discharge and observed suspended matter concentrations during sampling corresponds to 0.7 (±0.1, 1SD) t km^{-2} yr^{-1} (Table 2). Due to the highly variable, stochastic nature of suspended sediment transport (Kirchner et al., 2001; Schaller et al., 2001; Chalov et al., 2014), this estimate may not be representative. Sampling derived erosion rates for the Barguzin, the Selenga and the Upper Angara are, however, broadly consistent with the rates derived from times series. Denudation rates calculated from dissolved meteoric $^{10}Be/^{9}Be$ ratios (D_{Be}, Eq. (4)) range from 15.5 (±4.5, 1SD) t km^{-2} yr^{-1} in the Upper Angara catchment to 34.7 (±11.5, 1SD) t km^{-2} yr^{-1} in the Selenga catchment. For the Selenga, these Be-derived denudation rates exceed the summed chemical weathering and physical erosion rates by a factor of 4.3 (D_{Be}/D_{E+W}), while D_{Be} is lower in the Upper Angara catchment ($D_{Be}/D_{E+W} = 0.4$). In the Barguzin river catchment both denudation rate estimates are similar ($D_{Be}/D_{E+W} = 0.8$).

3.2. Lake data

Conductivity and alkalinity are rather uniform with depth in the lake (Fig. 2), but ~ 20% lower than the dis-

charge weighted river averages (corrected for seasonal variation). The variability in alkalinity is larger in surface waters than at depth. The pH at the lake surface is elevated compared to the riverine inputs (~8.4 vs. 7.8) but decreases with depth to, or even below, the discharge weighted river value.

The concentration and isotope composition of Sr is uniform with depth, and the same in all basins (Fig. 3). Sr concentrations are similar between rivers and the lake (~20% lower in the lake). For Be and Nd, there is variability in the isotope composition between the different basins. $^{10}Be/^{9}Be$ ratios are highest in the Southern and lowest in the Central Basin. For Nd, the Northern Basin is clearly the least radiogenic (ε_{Nd} of −14.2 to −13.1), while the other two basins have similar Nd isotope compositions (−9.0 to −7.7). The concentrations of Be and Nd are much lower in the lake compared to the rivers (~5% and ~ 1% of the discharge weighted river averages). Be concentrations also vary with depth, although the patterns show some variability between the different stations.

The isotope composition of the lake differs from the elemental flux weighted average of the tributaries for all three elements. $^{10}Be/^{9}Be$ is on average higher in the lake compared to the riverine input. Neodymium in the lake is less, and Sr slightly more, radiogenic (supplementary Fig. S1 in supplement S3).

3.3. REE patterns in the rivers and the lake

Post-Archean Australian Shale (PAAS) normalized REE patterns (Taylor and McLennan, 1985) for river and lake water samples are displayed in Fig. 4. The Selenga, Turka, and Barguzin rivers are slightly depleted in LREE. However, the Upper Angara and Kichera rivers show a LREE enrichment.

REE concentrations in the lake surface are 9 (Lu, Yb, Tm) to 41 times (Ce) lower than in the rivers. Concentrations further decrease with depth within the lake. Simultaneously, LREE depletion increases with decreasing concentration (i.e. with depth). The deepest sample in the Central Basin is exceptional and shows the highest observed concentration in the lake.

3.4. Core-top sediments

The detrital silicate sediment phases have distinct Nd and Sr isotope compositions in the three basins (Table 3). The Northern Basin sediments, and the sediments on top of the Academician Ridge separating it from the Central Basin, clearly have the least radiogenic Nd and most radiogenic Sr signatures. The core top sediment sample from the west coast of the Northern Basin (sample 10–12) is particularly extreme, with ε_{Nd} of –23.6 ± 0.2 and $^{87}Sr/^{86}Sr$ of 0.7702. The Central Basin sediments have the most radiogenic Nd isotope signatures (supplementary Fig. S1). The Central and Southern Basins have similar sedimentary Sr isotope compositions, with the Central Basin being slightly less radiogenic on average. The sample closest to the Selenga Delta (13-20b) has isotope compositions similar to the measured dissolved riverine values (ε_{Nd} of −5.0 ± 0.2 and $^{87}Sr/^{86}Sr$ of 0.7081; Table 1). The Sr isotope composition of the core top sample close to the mouth of the Upper Angara (13-19A) is similar to the riverine dissolved value ($^{87}Sr/^{86}Sr$ of 0.7080).

4. DISCUSSION

4.1. Source apportioning of dissolved weathering fluxes

Riverine dissolved fluxes derive from chemical weathering of different rock types as well as atmospheric inputs. Estimates of the relative contribution of these sources, and in particular of silicate weathering, are an important part of understanding how Lake Baikal reflects processes in its catchment. To apportion the riverine dissolved fluxes, we follow Négrel et al. (1993) and Gaillardet et al. (1999) using a simple inverse model based on element ratios of Ca, Mg, Sr, HCO_3^-, and Cl to Na, as well as Sr isotopes. Information on the setup of the inverse model, quality and gain analysis, as well as the *a priori* values used and

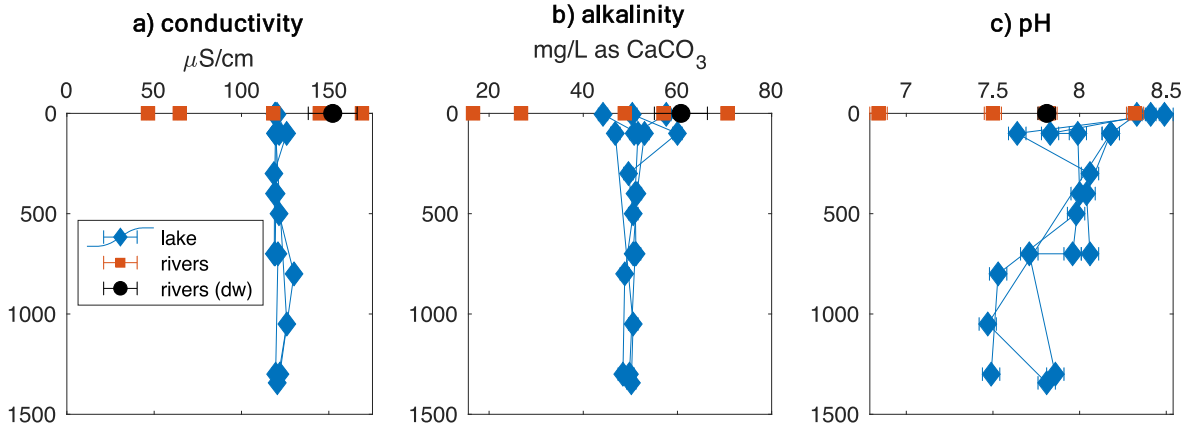


Fig. 2. Physico-chemical parameters in Lake Baikal and its major inflowing rivers. Symbols denote lake and river samples (key in a), "rivers (dw)" refers to the discharge weighted average composition of the measured rivers. For conductivity and alkalinity, rivers (dw) was corrected for seasonal effects, i.e. dilution at high discharge (see Section 2.3).

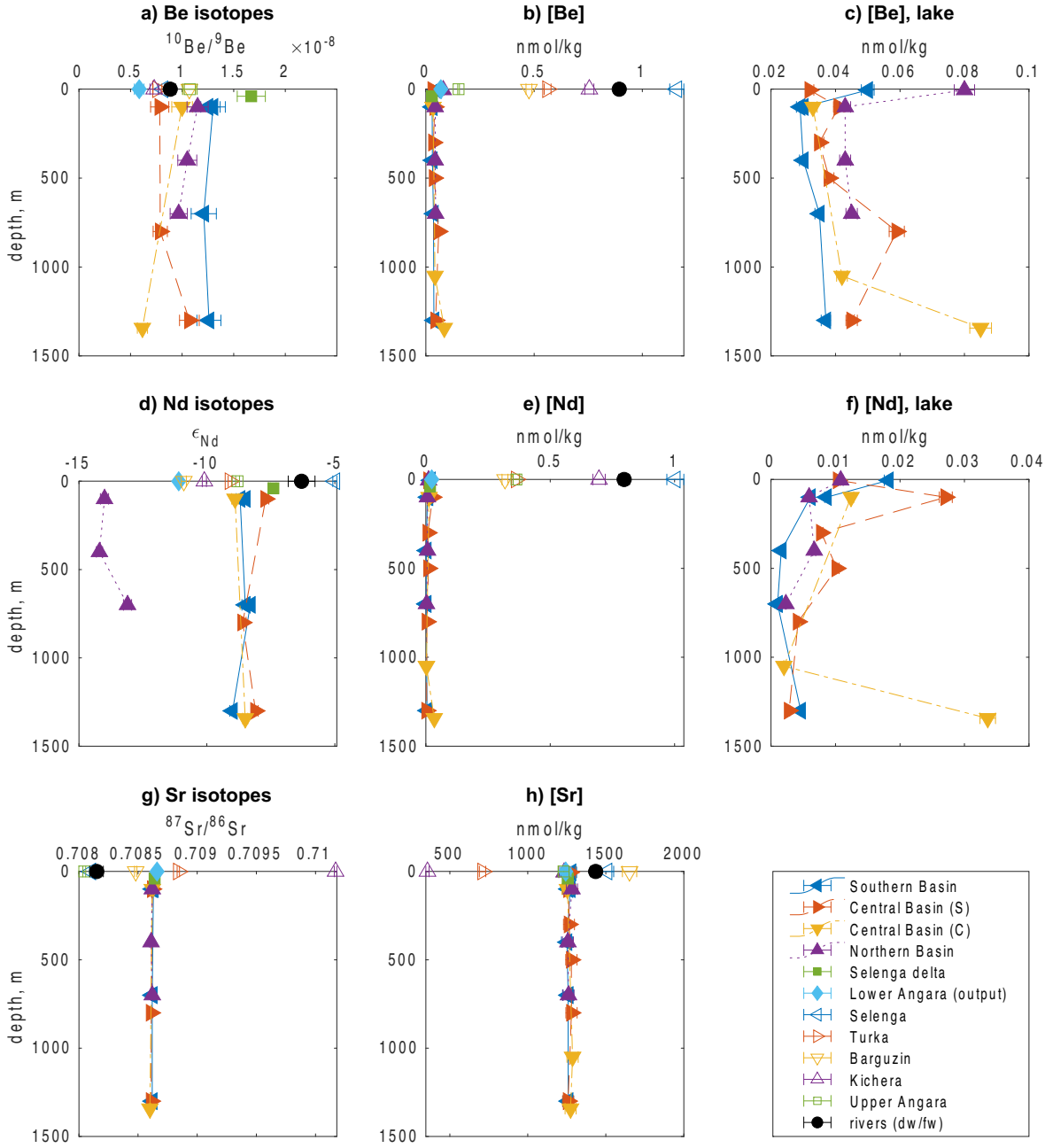


Fig. 3. Dissolved phase Be, Nd, and Sr concentrations and isotope compositions for tributaries and lake profiles in the three different basins. Panels c) and f) do not show the river data. The legend applies to all panels. "rivers (dw/efw)" refers to the river *discharge weighted* elemental concentrations and river *elemental flux weighted* isotope compositions. For Be, Nd, and Sr, uncertainties on the isotope composition of the bulk riverine input were deduced from estimates of seasonal variability, and the uncertainties on measured elemental concentrations and on the discharge of each river using available time series (Potemkina, 2011). Seasonal variability of isotope composition was estimated from small rivers for Nd (2 SD < 0.6 ε-units; Rickli et al., 2013; Rickli et al., 2017), from the seasonal variation found in the Yenisei River for Sr (annual range of ~ 0.00016, 2SD = 0.00008 used here; Hindshaw et al., 2019), and from measurements of the Be isotope composition of reactive phases in the Amazon river during and after the high discharge season (Wittmann et al., 2018).

the *a posteriori* values derived from the model are presented in supplement S2. The results of the inverse model for each river are presented in Table 4 and Fig. 5. Water samples were taken during high discharge season to maximize representativeness of the measured TDS parameters. However, we emphasize that this interpretation is drawn from a single water sample per river, and should therefore be understood as a snapshot that might not be completely representative of long-term weathering fluxes within the watersheds.

Bicarbonate derived from atmospheric CO_2 is a large contributor to the dissolved flux (26–32 mol%, 31–40 mass%) of these Baikal rivers, consistent with other obser-

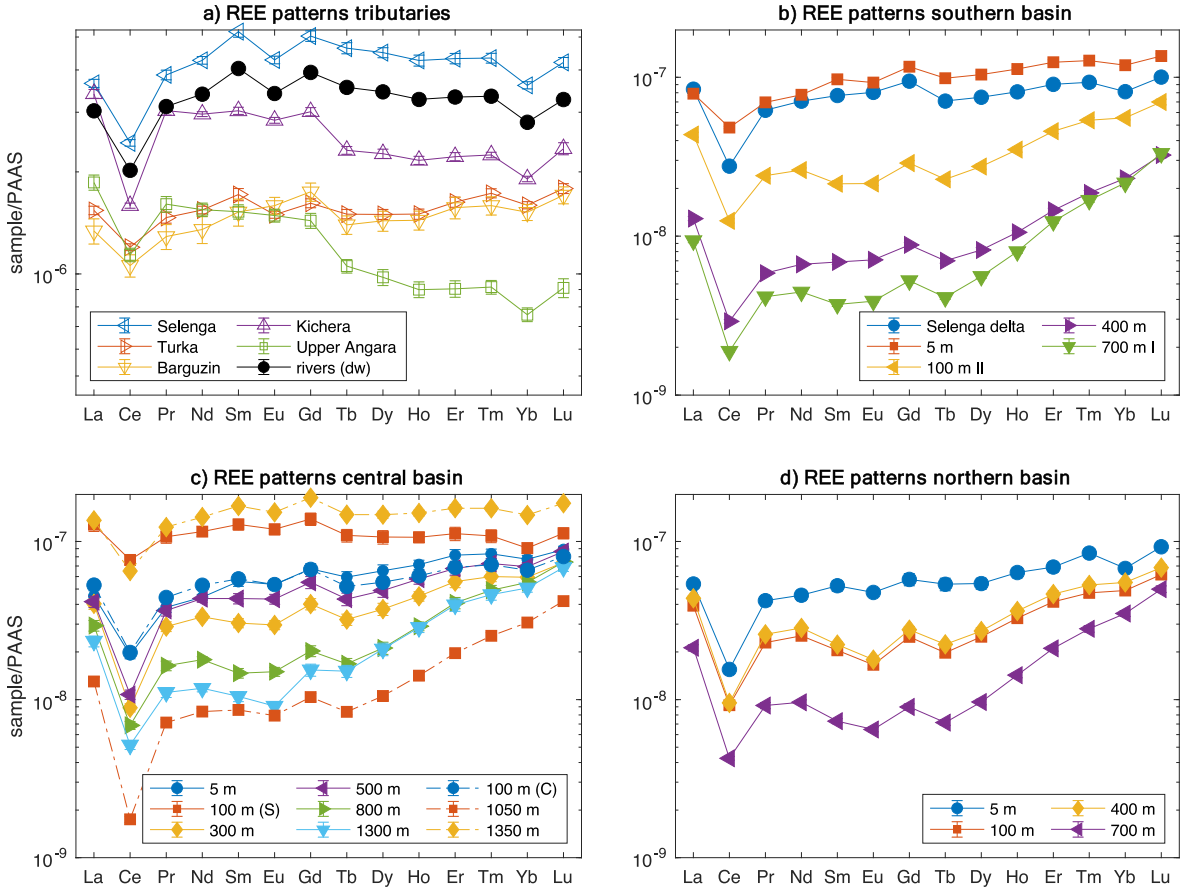


Fig. 4. PAAS normalized dissolved phase REE patterns for the studied tributaries of Lake Baikal (a), and for different depths within Lake Baikal for the Southern Basin (b), the Central Basin (c), (solid lines refer to station CB-C, stippled lines to station CB-S), and the Northern Basin (d). "rivers (dw)" refers to the weighted composition of the measured rivers.

vations in Siberia (e.g. Lena, Yenisei, Kolyma; Gaillardet et al., 1999). This likely relates to the low TDS, ranging from 44.2 (±3.8) to 119.8 (±9.2) mg L^{-1} compared to median and average TDS of 188 mg L^{-1} and 284 mg L^{-1} in large rivers (Gaillardet et al., 1999). Weathering derived solute fluxes are, hence, relatively low (further discussed in the next sections). The contribution of rain to the dissolved flux is small (<1.3 mol%) for all rivers, mainly due to the large distance of Lake Baikal from the ocean (>1600 km). Weathering of evaporites is negligible in all watersheds except in the Turka and Kichera, where it contributes 6.1 mol% and 2.1 mol% to the cation flux (and 4.9 mol% and 1.7 mol% to the total dissolved flux). To our knowledge, no evaporite lithologies are found in these catchments (Petrov et al., 2007), so that this small evaporite-assigned contribution might more likely reflect pollution.

Overall, the high contribution of carbonate weathering to the dissolved cation loads (58 to 78 mol%) and dissolved loads (46 to 64 mol%) is surprising given the large-scale geology of the region and the minor carbonate occurrences in the Selenga, Barguzin, Upper Angara, and Kichera catchments (Petrov et al., 2007). Although inverse model results from other rivers, e.g. the Congo (Négrel et al., 1993), also yield unexpectedly large carbonate contributions compared to catchment lithology, further potential sources of the high carbonate weathering proportions need to be explored. If dust fluxes to Lake Baikal apply to the river catchments (Agafonov, 1990; Anokin et al., 1991; Tarasova and Mescheryakova, 1992; as cited in Granina, 1997), this explanation would require the dust to have a high carbonate content, i.e. ~ 20% to account for 20% of the carbonate weathering flux. Alternatively, it may be that chosen lithological endmember compositions do not accurately reflect the setting of Lake Baikal. In the climate of Lake Baikal, Ca-rich plagioclase dissolves much faster than K-feldspar (Brantley, 2003; Goldberg et al., 2010), and is also a common mineral in lake sediments (~20–40%; Fagel et al., 2007) and surrounding lithologies. As a result, there could be a substantially higher Ca flux from silicate weathering than the inversion suggests based on a typical silicate Ca/Na ratio of 0.35 (Gaillardet et al., 1997; Gaillardet et al., 1999). For example, changing the composition of the silicate endmember to Ca/Na = 1 ± 0.15 (from 0.35 ± 0.15), decreases the inversion-derived contribution of carbonate weathering to Ca fluxes from 82–93% to 59–82% and the contribution to the dissolved cation load from 58-78 mol% to 44–71 mol%.

Silicate weathering contributes 20 to 42 mol% to the dissolved cation loads, though this could be higher given the

Table 4
Inversion-derived estimates of the *molar* fraction of the dissolved load reflecting silicate, carbonate, and evaporite weathering, as well as contributions from rain and atmosphere (HCO_3^-). Error estimates correspond to 1SD.

	silicate	carbonate	evaporite	rain	atmosphere
Selenga	20.6% ± 1.2%	49.2% ± 8.2%	0.3% ± 0.1%	1.1% ± 0.2%	28.8% ± 6.4%
Turka	15.1% ± 0.9%	46.0% ± 8.2%	4.9% ± 0.6%	1.9% ± 0.1%	32.1% ± 6.4%
Barguzin	9.2% ± 0.5%	63.9% ± 12.4%	0.0% ± 0.0%	0.8% ± 0.1%	26.0% ± 9.2%
Kichera	14.8% ± 0.9%	50.0% ± 8.0%	1.7% ± 0.3%	1.1% ± 0.4%	32.4% ± 6.4%
Upper Angara	11.3% ± 0.7%	56.5% ± 10.2%	0.2% ± 0.1%	1.3% ± 0.2%	30.6 ± 7.8%

above discussion (28 to 54 mol% using $Ca/Na_{sil} = 1$). The silicate weathering contribution to dissolved fluxes in the Selenga River (15 mass% and 21 mol% of the total chemical flux, 35 mass% and 42 mol% of the cation flux) is close to the median of the dataset for large rivers (Gaillardet et al., 1999), suggesting that it is representative in a global context. Lake Baikal, in turn, receives ~ 50% of river inflow from the Selenga River (Afanasjev, 1976; Leibovich-Granina, 1987; as cited in Seal and Shanks, 1998), rendering the lake a representative archive of global weathering processes in terms of lithological sources.

4.2. Chemical weathering, physical erosion, and total denudation rates in the Lake Baikal watershed

The spatial patterns of chemical weathering and physical erosion rates are controlled by a complex array of processes and factors, including runoff, temperature, lithology, and slope. In this section, we analyze these factors and assess how the rivers around Lake Baikal compare to global average rates.

4.2.1. Magnitude of chemical weathering, physical erosion, and total denudation rates

On a global scale, *in-situ* ^{10}Be-derived estimates for denudation rates range from 141 to 235 t km^{-2} yr^{-1} (Larsen et al., 2014; Wittmann et al., 2020), consistent with compilations of TDS and suspended matter fluxes, yielding a global denudation rate of 222 t km^{-2} yr^{-1} (Milliman and Farnsworth, 2013; Wittmann et al., 2020). Denudation rates for Lake Baikal based on Be isotopes (D_{Be}) are much lower, ranging from 15.5 ± 4.5 (Upper Angara; 6 ± 2 mm kyr^{-1} assuming a rock density of 2.5 t m^{-3}) to 34.7 ± 11.5 t km^{-2} yr^{-1} (Selenga; 14 ± 5 mm kyr^{-1}). Similarly, denudation rates based on physical erosion and chemical weathering fluxes do not exceed 33.6 t km^{-2} yr^{-1}. Erosion rates deduced from timeseries data (Potemkina, 2011) fall below 5 t km^{-2} yr^{-1}. Although based on a high sampling frequency, they might nevertheless underestimate real fluxes due to the stochastic nature of sediment discharge (Kirchner et al., 2001; Schaller et al., 2001).

Models and compilations of riverine chemistry suggest a global average chemical weathering rate of 11–39 t km^{-2} yr^{-1} (Gaillardet et al., 1999; Milliman and Farnsworth, 2013; Hartmann et al., 2014). The values for the Turka, Barguzin, and Upper Angara rivers fall within this range (Table 2). Only the chemical weathering rate estimated for the Selenga River (5.7 ± 0.9 t km^{-2} yr^{-1}; 2.3 ± 0.4 mm kyr^{-1}) is lower, which is likely due to the low runoff in the Selenga catchment (Section 4.2.3). Irrespective of sediment storage processes discussed in Section 4.2.2, the low denudation rates observed at Lake Baikal are thus the

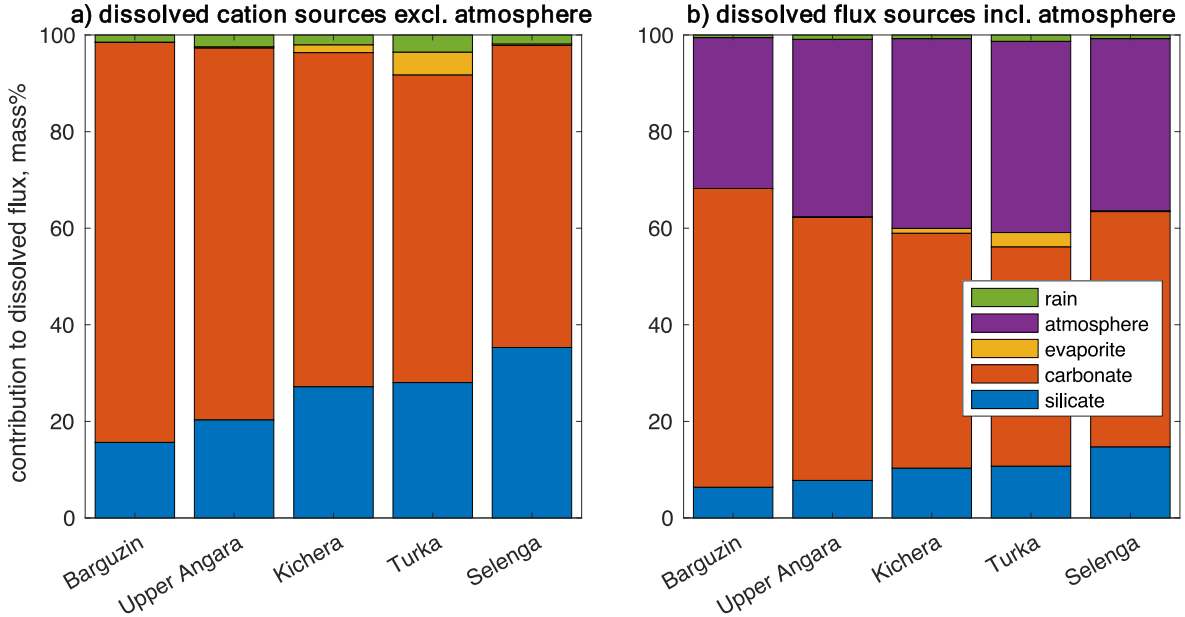


Fig. 5. Estimates of the relative contributions (by *mass*) of silicate, carbonate, and evaporite weathering as well as rain to the dissolved cation flux (a) and the total chemical flux (b) for the different tributaries. Atmosphere refers to atmosphere derived HCO_3^-.

result of low physical erosion, while chemical weathering rates are similar to the global rate.

4.2.2. Comparison of denudation rates derived from river loads and meteoric Be isotopes

Denudation rates (D_{E+W}), estimated from chemical weathering and physical erosion rates, are comparable with meteoric Be based denudation rates (D_{Be}) for the Barguzin River (Fig. 6 and Fig. 7a). For the Selenga, D_{E+W} is much lower than D_{Be}. A likely reason for this finding is that a large portion of the sediment eroded in the southerly watersheds does not reach the sampling site close to where the river enters the lake (Chalov et al., 2014). In this context, we interpret D_{Be} as the total denudation flux that is removed from most of the catchment, and D_{E+W} as the denudation flux that reaches the lake (or sampling location) after upstream sediment storage (SS) processes:

$$D_{Be} = D_{E+W} + SS \quad (5)$$

For the Selenga River, Chalov et al. (2014) have estimated that 90% of river-borne suspended matter is deposited, mainly in channels and overflow banks, in the downstream river system within 200 km distance of the Selenga Delta. Similarly, our data suggest that only ~ 25% of the erosion flux reaches our sampling location (~40 km before the lake, using recent erosion data from 1995–2005 from Potemkina, 2011), confirming the importance of sediment storage in the Selenga catchment. Sediment storage may also explain the large difference between D_{Be} and D_{E+W} in the catchment of the Turka. This conclusion is consistent with our preliminary finding of low E in this catchment (Table 2).

In the Upper Angara catchment, D_{E+W} exceeds D_{Be}. This could potentially reflect increased chemical weathering rates due to recent permafrost thawing (Section 4.2.3), which exceeds D_{Be} on its own (Fig. 6). These recent changes in chemical weathering are not reflected in D_{Be} due to its long integration time governed by the residence time of ^{10}Be in soils. For meteoric ^{10}Be, this timescale depends on denudation rates and the adsorption depth in soils (Willenbring and von Blanckenburg, 2010). In Central Siberia, the active layer in which permafrost thaws during summer, facilitating at least seasonal water percolation, ranges from 0 to 110 cm depending on season and orientation of the slope (Prokushkin et al., 2007; Bagard et al., 2011; Bagard et al., 2013). Thus, a ^{10}Be soil adsorption depth range of 5 cm (~winter conditions) to 50 cm (~50 cm being the annual active layer depth average) might reflect realistic permafrost conditions. For the denudation rates observed here, the ^{10}Be integration timescale would be 2500 to 5000 yrs for a ^{10}Be soil adsorption depth of 5 cm, and 25 to 50 kyrs for a soil adsorption depth of 50 cm (Willenbring and von Blanckenburg, 2010).

Another caveat in comparing different approaches for estimating denudation rates, unrelated to variable integration time scales, is the uncertainty on our D_{Be} estimates. In particular, there are no local estimates for the mobile fraction of Be. In addition, the estimate of the atmospheric ^{10}Be flux relies on global circulation models (Heikkilä and Smith, 2013; Heikkilä et al., 2013; Heikkilä and von Blanckenburg, 2015), which may not necessarily accurately reflect the real flux.

4.2.3. Spatial distribution of chemical weathering, physical erosion, and total denudation rates

Chemical weathering shows a clear trend from low rates in the south (Selenga) to high rates in the north (Upper Angara; Fig. 6), which could be related to several factors. First, the trend could be driven by the first order effect of runoff on chemical weathering rates (e.g. White and Blum, 1995; Gislason et al., 2009; Hartmann, 2009, Fig. 7a), as runoff increases from ~ 60 mm yr^{-1} in the Selenga catchment to 380 mm yr^{-1} for the Upper Angara in the North. Second, the northern part of the catchment was more heavily affected by glaciation during the last ice age (e.g. Karabanov et al., 1998). Potentially, the northern catchments still host fine, glacially-produced sediments of high reactivity that lead to high weathering rates today. Third, the average slope (as extracted from GIS analysis

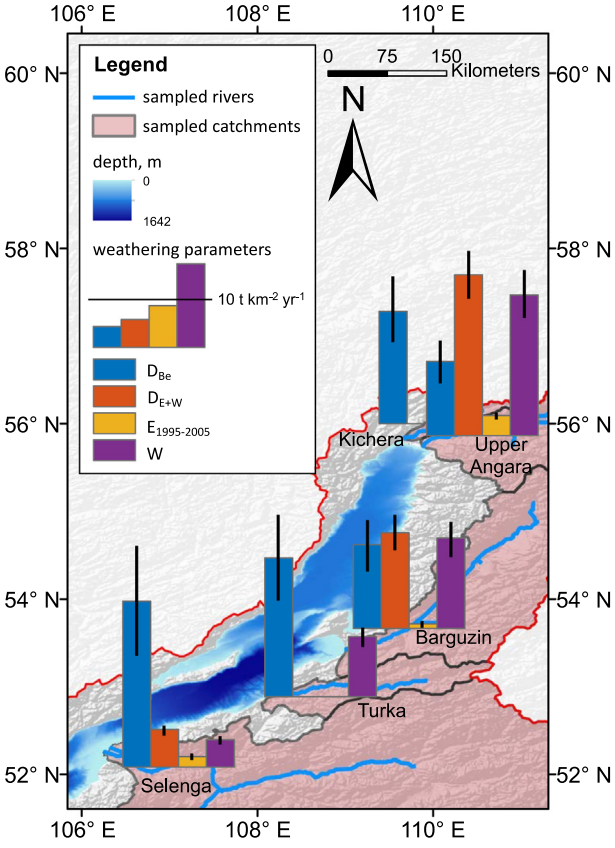


Fig. 6. Estimates of denudation, chemical weathering (W), and physical erosion rates for the sampled tributaries of Lake Baikal. Both the Be isotope based estimates (D_{Be}), as well as the physical erosion and chemical weathering based estimates of denudation rates are shown (D_{E+W}). Erosion rates are based on sediment fluxes between 1995 to 2005 ($E_{1995-2005}$), thought to more or less reflect natural erosion fluxes (Potemkina, 2011; Chalov et al., 2014). No time series data is available for the Turka and Kichera rivers. For the Kichera River, the missing annual water discharge data prevents the calculation of weathering and physical erosion rates. Error bars = 1SD. Erosion data from Potemkina (2011).

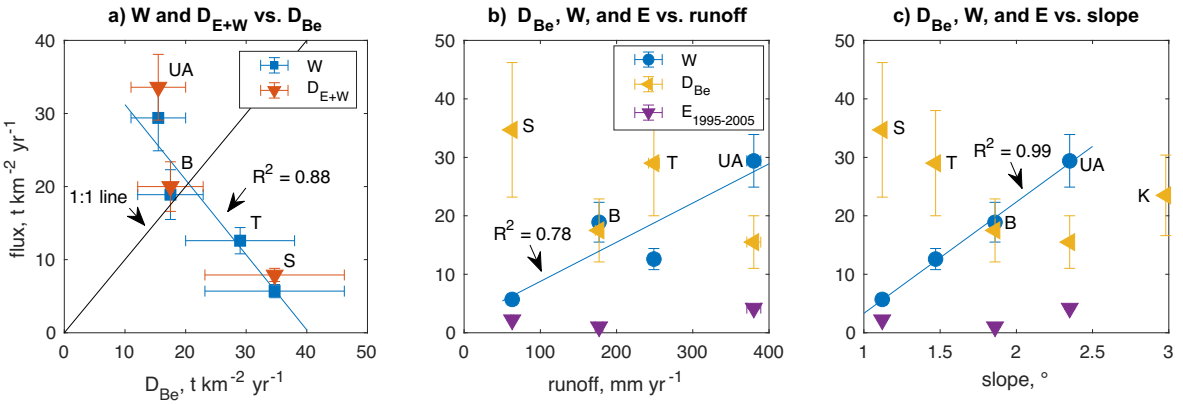


Fig. 7. Relationship of denudation, weathering, and erosion rates ($E_{1995-2005}$) with runoff (a) and slope (b). Chemical weathering rates show a clear correlation with runoff and slope, which is not the case for erosion and Be-based denudation rates (see discussion). Panel c) shows the relationship between weathering (W) and denudation rates (D_{E+W}; based on the sum of W and erosion rates $E_{1995-2005}$), and D_{Be}. Both W and D_{E+W} (dominated by W) are negatively correlated with D_{Be}, likely due to the cumulative effect of permafrost (recent thawing, stabilization of erosion; see discussion). River catchments with $D_{E+W} < D_{Be}$ (falling below the 1:1 line) are interpreted to exhibit sediment storage within river systems. Data points with the same x-value correspond to the same river (S = Selenga, T = Turka, B = Barguzin, UA = Upper Angara, K = Kichera). Erosion data from Potemkina (2011).

in ArcGIS) of the sampled catchments also increases towards the north (Fig. 7b). Physical erosion rates typically increase with slope (Ahnert, 1970; Montgomery and Brandon, 2002; Ouimet et al., 2009; Bufe et al., 2021). As a result, the higher chemical weathering rates in the north could be sustained by the supply of fresh, unweathered material (although this would need to be retained within the river catchments, see below). Fourth, the trend could also be driven by changes in lithology, in particular the occurrence of carbonate rocks. This would also agree with the results of the river water inversion indicating higher carbonate derived weathering fluxes in the northern catchments (Fig. 5).

With increasing slope and runoff, one would expect physical erosion rates to also increase towards the north. Surprisingly, this is not the case (Figs. 6 and 7). Furthermore, D_{Be} is lower in the north than in the south resulting in a negative correlation with chemical weathering rates (Fig. 7c). We hypothesize that the reason for this could be that permafrost in the northern regions stabilizes soils and prevents erosion, but that recently increased permafrost thawing and deepening of the active layer may have elevated dissolved fluxes (MacLean et al., 1999; Frey et al., 2007; McClelland et al., 2016; Colombo et al., 2018) due to increased water–solid phase interactions (Bring et al., 2016) and groundwater contributions (Frey and McClelland, 2009; Walvoord et al., 2012). Such an increase of active layer depth has, for example, been observed in the Siberian Yenisei river catchment (Hindshaw et al., 2019) and may be particularly pronounced for the Upper Angara catchment.

4.3. Removal of trace elements at the river-lake interface and in the lake

4.3.1. Magnitude of removal

A key uncertainty in relating records of ocean chemistry to sources such as continental chemical weathering is the extent to which riverine fluxes are modified at the continent-ocean boundary (e.g. Boyle et al., 1974; Boyle et al., 1977; Sholkovitz, 1978). The importance of this process must also be assessed for Lake Baikal. The concentrations of many trace elements are also much lower in Lake Baikal compared to the river discharge weighted average (Fig. 3, Fig. 4, and supplement S4). We quantify the removal of river supplied elements from the difference in concentration between lake and rivers:

$$removal, \% = \left(1 - \frac{c_{i,river}}{c_{i,lake}}\right) * 100 \quad (6)$$

where $c_{i,river}$ is the discharge weighted average riverine concentration of element i, and $c_{i,lake}$ is its concentration in the lake, calculated using all lake measurements, and taking into account the volumes of different depth intervals (Sherstyankin et al., 2006).

As shown in Table 5, the greatest removal is observed for Be (95%), Mn (97%), Y (98%), REE (98–99%), and Fe (99.6%). The small amount of removal calculated for major elements like Mg, K, and Ca, is expected given their conservative nature and consistent with previous findings at Lake Baikal (Falkner et al., 1997). The only element for which no removal occurs is Pb, which has higher concentration in the lake, most likely due to additional sources of Pb to the lake (e.g. from pollution).

Removal of Be and Fe at Lake Baikal is greater (95 and > 99%) than the average estimated at the river-ocean interface, corresponding to ~ 55% (Suhrhoff et al., 2019) and ~ 90%, respectively (Poulton and Raiswell, 2002; and references therein). Similarly, only 20 to 45% of Mn is lost in mixing experiments of river and ocean water (Sholkovitz, 1978), whereas 97% is removed at Lake Baikal. Although REE removal in estuaries can be very strong, ranging from 86% for Lu to 95% for La in the Amazon estuary (Sholkovitz, 1995), global scale removal is estimated at 70% for Nd (Rempfer et al., 2011; Rousseau et al., 2015),

Table 5
Removal at the river lake interface and within the lake, lake inventories, riverine fluxes, and residence times of elements analyzed in this study. Lead concentrations are higher in the lake than in the rivers, most likely due to pollution (see discussion).

	Removal (%)	Riverine flux (mol/yr)	Lake inventory (mol)	Residence time (yrs)	Published[a] residence time (yrs)
	I. (trace) elements, sorted by residence time				
Pb	−186.2	$2.13 * 10^4$	$2.49 * 10^7$	1170	
Mo	9.2	$9.47 * 10^5$	$3.51 * 10^8$	371	
Sr	18.7	$9.01 * 10^7$	$2.99 * 10^{10}$	332	370.0
Mg [b]	20.5	$9.20 * 10^9$	$2.99 * 10^{12}$	325	320.0
Cr	23.4	$1.30 * 10^5$	$4.06 * 10^7$	313	320.0
K [b]	24.6	$1.89 * 10^9$	$5.81 * 10^{11}$	308	360.0
Rb	24.8	$5.11 * 10^5$	$1.57 * 10^8$	307	
Ca [b]	26.2	$3.19 * 10^{10}$	$9.63 * 10^{12}$	302	330.0
Li	30.6	$2.50 * 10^7$	$7.08 * 10^9$	283	313.0
Ba	32.1	$6.52 * 10^6$	$1.81 * 10^9$	277	320.0
Na [b]	34.3	$1.34 * 10^{10}$	$3.59 * 10^{12}$	268	290.0
U	51.8	$2.14 * 10^5$	$4.21 * 10^7$	197	160.0
Re	55.9	$4.68 * 10^2$	$8.44 * 10^4$	180	
Ni	72.1	$5.32 * 10^5$	$6.06 * 10^7$	114	110.0
V	73.6	$1.46 * 10^6$	$1.57 * 10^8$	108	130.0
Cu	81.3	$8.55 * 10^5$	$6.55 * 10^7$	76.6	94.0
P	82.6	$3.95 * 10^7$	$2.80 * 10^9$	71.0	
Si	86.0	$1.04 * 10^{10}$	$5.94 * 10^{11}$	57.2	170.0
Be	95.3	$5.12 * 10^4$	$9.78 * 10^5$	19.1	
Mn	97.3	$5.62 * 10^6$	$6.19 * 10^7$	11.0	
Y	98.0	$8.26 * 10^4$	$6.77 * 10^5$	8.2	
Fe	99.6	$1.06 * 10^8$	$1.86 * 10^8$	1.8	
	II. REE				
La	98.5	48,136	299,549	6.2	
Ce	99.1	66,376	237,281	3.6	
Pr	98.9	11,304	50,960	4.5	
Nd	98.8	46,090	225,565	4.9	
Sm	99.0	8615	35,956	4.2	
Eu	98.9	1399	6570	4.7	
Gd	98.8	6729	34,242	5.1	
Tb	98.9	1006	4611	4.6	
Dy	98.8	5738	29,268	5.1	
Ho	98.5	1135	6916	6.1	
Er	98.3	3269	22,787	7.0	
Tm	98.2	464	3481	7.5	
Yb	97.9	2640	22,562	8.5	
Lu	97.8	473	4331	9.2	

[a] (Falkner et al., 1997).
[b] Riverine flux corrected for seasonal variation, i.e. dilution at high discharge (see Section 2.3; Meybeck, 2003; Zakharova et al., 2005). This was not done in Falkner et al. (1997); our residence times estimates for these elements should be increased by ~ 10% for a direct comparison.

far lower than the 98 to 99% observed in this study. Removal of trace elements in lakes is less well studied but is, for example, demonstrated by lower concentrations of a range of elements (e.g. Be, V, Ni, Zn, Cd, Pb, U) in river outlets of Swedish lakes compared to their inlets (Temnerud et al., 2013) as well as decreasing concentrations of Fe, Cu, and As with distance to the river mouth in a Pakistani lake (Imran et al., 2021).

4.3.2. Causes of removal

Many different processes, such as changes in dissolved-adsorbed partitioning, colloid dynamics, uptake by organisms, and the formation of authigenic phases, can remove trace elements from solution. These processes are extremely complex and often interdependent, and a rigorous identification of the controlling processes is difficult. Quantitative apportioning of the sinks goes beyond the scope of this study and would, for example, require a lacustrine "estuary" transect or mixing experiments as well as a higher spatial sample density in general. However, removal processes are an important part of understanding the relationship between a lake or a marine record and the supply of material from the continents by chemical weathering and rivers, and we briefly discuss the potentially relevant processes.

4.3.2.1. Conductivity and organic colloids. As conductivity of lake water is slightly lower than the discharge weighted average of the rivers (Fig. 2a), contrasting with strong salinity increases across marine estuaries, salinity-induced coagulation and settling of colloidal (organic) matter and trace

elements bound to them (e.g. Boyle et al., 1974; Boyle et al., 1977; Sholkovitz, 1978; Gustafsson and Gschwend, 1997; Fitzsimons et al., 2012) cannot be the mechanism by which trace elements are removed at Lake Baikal. Nevertheless, organic colloid dynamics may be a possible driver of trace element removal. Organic colloids have very large specific surface areas that host a variety of negatively charged functional groups, making them efficient carriers of trace elements (Gustafsson and Gschwend, 1997). Yoshioka et al. (2002) observed that DOC concentrations (as a proxy for organic colloids) in Lake Baikal are 4–5 times lower than in its inflowing rivers. If this DOC decrease were associated with the loss of riverine suspension at the river-lake interface, organic colloids could still be key for trace element removal. Organic carbon dynamics also have a large impact on the removal of many trace elements found in Swedish lakes (Temnerud et al., 2013).

4.3.2.2. pH induced adsorption at the river-lake interface. The equilibrium partitioning between the dissolved phase and a pool absorbed to the surfaces of particulate oxides (and organic colloids) is pH-dependent, with higher pH leading to greater adsorption (e.g. Schindler and Stumm, 1987; Drever, 1998). As a result, for example, riverine Nd concentrations are inversely correlated with pH (Deberdt et al., 2002). For REE, the significance of pH for removal processes has also been demonstrated in laboratory experiments (next section; Sholkovitz, 1995), and elevated pH has been suggested to cause removal in Swedish lakes (Temnerud et al., 2013). Similarly, at Lake Baikal, mixing of lake (pH ~ 8.4 at the surface) and river water (discharge weighted average pH of 7.8) could lead to the removal of trace elements from solution. This hypothesis gains further support from an in-depth analysis of the change in REE patterns at the river-lake interface. REEs tend to fractionate during adsorption processes, with a higher fraction of LREE adsorbing to surfaces compared to heavy REE (HREE; e.g. Sholkovitz, 1995). Increased LREE depletion in the lake surface compared to the riverine inputs is apparent in changing REE patterns (Fig. 4), resulting in a decrease of normalized La to Yb ratios ($(La/Yb)_n$, see caption to Fig. 8a for details) from 1.3 in the rivers to 0.8 in the lake (samples < 500 m). The equilibrium timescale for this process is rather short, i.e. a few days for e.g. Be (You et al., 1989) and less than a day for Nd (Sholkovitz, 1995), such that the majority of this removal should occur close to the river-lake interface. The calculated removal, however, integrates processes that occur at the river-lake interface and additional removal processes occurring within the lake (next section), which may also explain why the observed removal exceeds typical removal in marine estuaries.

4.3.2.3. Removal in the lake through the formation of authigenic phases. The evolution of REE patterns and Ce anomalies (Ce*) with depth in the lake provides further insights into removal processes and the formation of lacustrine authigenic phases. For example, negative Ce* can be indicative of the involvement of freshly forming Fe-Mn (oxyhydr)oxide surfaces during the removal of REE due to their ability to oxidize Ce(III) to insoluble Ce (IV) (e.g. Moffett, 1994; Bau, 1999). Ce anomalies were calculated as in Sholkovitz (1995):

$$Ce^* = \frac{3Ce_n}{(2La_n + Nd_n)} \quad (7)$$

where n refers to Post-Archean Australian Shale (PAAS) normalized ratios (Taylor and McLennan, 1985). Values

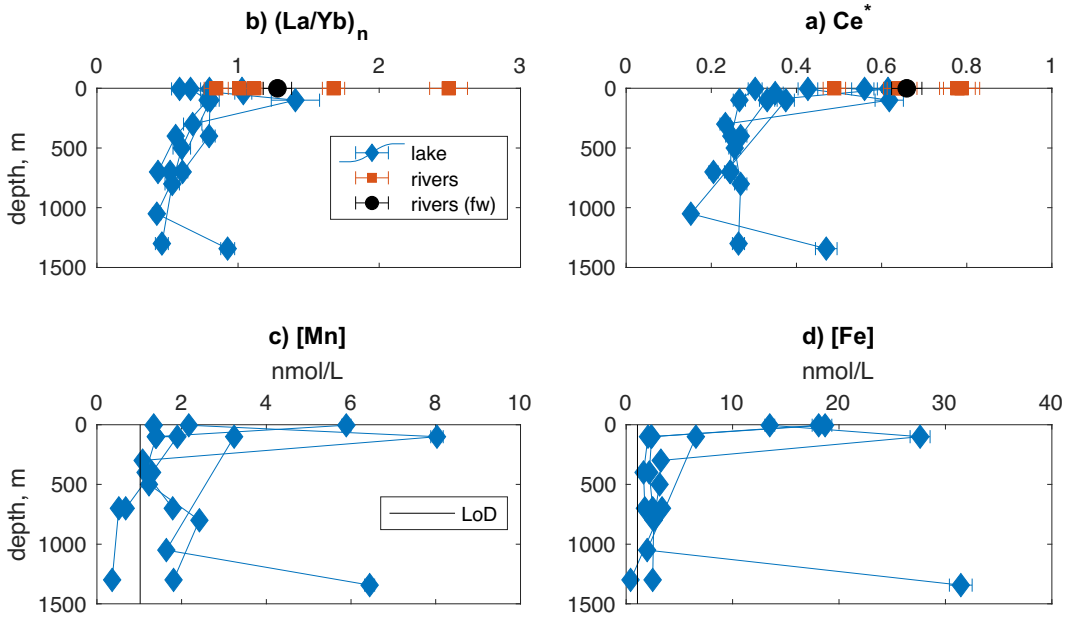


Fig. 8. PAAS normalized dissolved La to Yb ratios $(La/Yb)_n$ (a; calculated as La_{sample}/La_{PAAS} divided by Yb_{sample}/Yb_{PAAS}), Ce anomalies (b), as well as Fe and Mn concentrations (c, d), in Lake Baikal and its major inflowing rivers. Symbols denote lake and river samples (key in a), "rivers (dw)" refers to the discharge weighted composition of the measured rivers. LoD denotes the analytical limits of detection for Fe and Mn concentrations.

below 1 indicate Ce depletion relative to its neighboring elements and are referred to as "negative" anomalies. Ce anomalies are shown in Fig. 8b.

Negative Ce anomalies develop at depth in the lake and REE patterns become increasingly LREE depleted (though La seems to be removed less than other LREE; Fig. 4). At the same time, Fe and Mn concentrations decrease (Fig. 8c and d), together with REE (Fig. 4), Y, and U concentrations (supplement S4). This suggests progressive adsorption or incorporation of these elements into freshly forming authigenic Mn and Fe-Mn oxides and hydroxides (Moffett, 1994; Bau, 1999; Schijf et al., 2015), contributing to their removal from lake water. The formation of new Mn and Fe-Mn oxyhydroxide coatings on particulate material may also explain why there is no release of trace elements associated with the drop in pH with depth within the lake.

4.4. Residence times and lake budgets

4.4.1. Residence times and mixing of Sr, Be and Nd

The residence times of elements in the lake determine how quickly the chemistry of the lake responds to changing inputs and how variable concentrations and isotope compositions of elements are throughout the lake. Both are important for the interpretation of paleo-weathering records, and determine whether sediment cores record local signals or changes to the chemistry of the whole lake. The lake residence times of major cations (Mg, K, Ca, and Na) and soluble trace elements (e.g. Sr, Rb, Mo) can be calculated by dividing the lake inventory by the riverine flux, based on the assumption that there is no significant removal process for these elements at the river-lake interface. These residence times are in the range of 300 to 370 years (except Na with ~ 270 yrs; Table 4), in broad agreement with the estimates of Falkner et al. (1997). Since this is similar to the water residence time, these elements are primarily removed through outflow of water from the lake. While it is clear that deep water is renewed on a timescale of 8 to 18 years in each basin (Falkner et al., 1991; Weiss et al., 1991; Hohmann et al., 1997; Peeters et al., 1997), indicative of intra-basin mixing, it is currently not clear to what extent the different basins mix and, if so, on what time scale. The uniform distribution of Sr isotopes in the lake (Fig. 2 g) clearly shows that mixing of the whole lake must occur on a time scale much shorter than the residence time of Sr (~330 years).

Estimating lake residence times for particle-reactive elements is more complicated, because the relative magnitude of removal at the lake–river interface and within the lake remains uncertain (Section 4.3.2). Minimum total lake residence times for REE, assuming no "estuarine" removal, range between ~ 4 and ~ 10 yrs. The minimum residence time for Be is ~ 20 yrs (Table 5). For these elements, the interior lake residence times are likely longer due to removal processes at the lake interface. Consistent with the inferred removal processes in the water column (Section 4.3.2.3), residence times similar to Sr can, however, be precluded given the isotopic variability between the basins in Be and Nd isotope compositions (Fig. 2).

4.4.2. Missing sources of Sr, Nd, and Be

4.4.2.1. Missing source of Sr and Nd. The different isotope composition of the lake compared to the measured riverine inputs (Fig. 3) suggests that there are sources of Nd, Sr, and ^{10}Be to the lake which were not identified in our sampling campaign. To assess how representative the fluxes of Nd, Sr, and Be measured here are for total riverine inputs, we calculate the flux of the missing Sr and Nd using a mixing model:

$$R_{Y,lake} = \sum_i R_{Y,i} f_{Y,i} \tag{8}$$

where $R_{Y,i}$ refers to the isotope composition of element Y (Sr or Nd) in a flux i (i = rivers, dust, missing source), $f_{Y,i}$ is the fraction of element Y delivered from flux i, and $R_{Y,lake}$ is the isotope composition of element Y in lake. Seasonal variability in riverine isotope compositions are small compared to the range of measurements and estimates for the isotope composition of the missing source at Lake Baikal, in particular for Nd and Be (Tipper et al., 2006; Rickli et al., 2013; Rickli et al., 2017; Wittmann et al., 2018; Hindshaw et al., 2019). Although such variations are taken into account (see caption Fig. 3), they have no significant effect on our budget considerations. The mixing model is solved for the flux of the missing source using constraints on its isotope compositions derived from the detrital sediments in the Northern Basin and its surrounding lithologies (Gladkochub et al., 2009), which have matching unradiogenic Nd and radiogenic Sr signatures. Strontium and Nd dust fluxes and their isotope composition are estimated from dust mass fluxes (Agafonov, 1990; Anokin et al., 1991; Tarasova and Mescheryakova, 1992; as cited in Granina, 1997) as well as Sr and Nd concentrations, solubility, and isotope composition of loess from the Northern Chinese loess plateau (Yokoo et al., 2004). More details on the mixing model and its underlying observational constraints can be found in supplement S3. Based on the spatial homogeneity/variability (Fig. 2), the mixing model is applied to the entire lake for Sr, while the Northern Basin is considered separate from the combined Southern and Central Basin for Nd.

For Sr, the isotope budget can be almost entirely explained by the riverine inputs, which provide 94–99% of Sr to the lake (Table 6). Dust inputs are negligible (<1%), and the missing radiogenic source provides 0.8 to 5.8% of the Sr, the range reflecting the mentioned range of plausible Sr isotope compositions (0.7162 to 0.7702, see also supplement S3). For Nd, dust inputs are negligible in the Southern and Central Basins (<1%), but make up 4.1 to 5.5% in the Northern Basin. The missing unradiogenic source is more important in the Northern Basin (26.3 to 44.7%) than in the Southern and Central Basins (14.0 to 21.3%), which indicates that the main source is probably located in the Northern Basin.

A possible source could be hydrothermal springs, which occur within the Northern Basin, along the northeastern coast (e.g. Shanks and Callender, 1992; Kipfer et al., 1996) and at several locations around the Northern Basin on land, including the western shore (Falkner et al., 1997; Sklyarova et al., 2017). Constraining the isotope composi-

Table 6
Estimates of the contribution of rivers, dust, atmospheric wet and dry deposition, and a missing source to the total inputs of Sr, Nd, and ^{10}Be into Lake Baikal. Uncertainty ranges correspond to the range of isotope compositions assumed for the missing source (Sr and Nd), and to 1 SD for ^{10}Be.

Sources	Sr	Nd		^{10}Be		
		SB & CB	NB	SB	CB	NB
Rivers	94.0–99.0%	77.9–85.2%	51.2–68.2%	67.4% ± 6.4%	100% ± 22%	102% ± 9.6%
Dust	<1%	<1%	4.1–5.5%	-	-	-
Atmospheric wet & dry deposition	-	-	-	32.6% ± 6.4%	0% ± 22%	−2.1% ± 9.6%
Missing source	0.8–5.8%	14.0–21.3%	26.3–44.7%	-	-	-

tion of a putative hydrothermal endmember is difficult because there are no isotope measurements of lake-floor hydrothermal fluids. On land, Sr isotope compositions in hydrothermal springs are extremely heterogeneous (^{87}Sr/^{86}Sr of 0.7064 to 0.7235; Falkner et al., 1997). The detrital sediment from the northwest shore of the basin (core 10–12) may provide an estimate for hydrothermal fluids, under the assumption that these fluids integrate signatures of the country rocks in the northwest, similar to the sediments themselves. This core is also interesting because it originates from the tectonically active border fault zone close to Zavorotnyi, which forms a small tectonic subbasin (Matton and Klerkx, 1995; Hus et al., 2006) where hydrothermal springs might occur. If this relatively extreme sedimentary isotope signature was indeed representative of hydrothermal discharge and if hydrothermal discharge constitutes most of the missing source flux, the contribution to the lake basin budgets would be more towards the lower bound estimate (i.e. 26.3% of Nd in the Northern Basin). However, in the oceans, hydrothermal systems are a negligible source of Nd (Goldstein and Jacobsen, 1987; Bertram and Elderfield, 1993) or might even constitute a sink due to efficient scavenging within marine hydrothermal plumes (e.g. Michard et al., 1983; Stichel et al., 2018). If the same applies at Lake Baikal, as indicated by the overall removal of Nd from the water column, it would be questionable whether the missing Nd could be supplied to the lake by hydrothermal discharge.

Alternatively, the missing unradiogenic Nd could stem from riverine discharge in small streams draining Archean and Proterozoic lithologies outcropping around the Northern Basin and elsewhere (e.g. Heim et al., 2007) or benthic fluxes, known to be important for the marine budget of Nd (Lacan and Jeandel, 2005; Jeandel et al., 2011; Rempfer et al., 2011; Abbott et al., 2015). A detailed sampling campaign of hydrothermal springs and small rivers, and pore waters of sediment cores would be useful to identify the missing source.

4.4.2.2. Missing source of ^{10}Be. For ^{10}Be, the contribution from rivers was calculated from the elemental flux weighted average riverine ^{10}Be/^{9}Be ratios delivered to the respective lake basin. The remainder is assumed to derive from atmospheric wet and dry deposition.

$$f_{^{10}Be,rivers},\% = \frac{\left(\frac{^{10}Be}{^{9}Be}\right)_{rivers,fw}}{\left(\frac{^{10}Be}{^{9}Be}\right)_{lake}} * 100 \quad (9)$$

Assuming that half of the Selenga discharge flows into the Central Basin (and half into the Southern Basin), its Be isotope budget does not actually require atmospheric inputs (Table 6). The same is true for the Northern Basin based on the isotope composition of the Upper Angara, dominating over the Be flux of the Kichera. For the Southern Basin, 32.6% (±6.4%) of ^{10}Be are estimated to derive from atmospheric inputs.

The fact that elemental flux weighted riverine Be isotope compositions are similar to the lake composition in the Northern and Central Basins might suggest that additional riverine sources have lower ^{10}Be/^{9}Be ratios. This would also be consistent with the fact that many of the small rivers not sampled here drain mountainous catchments, presumably with high denudation rates (and low ^{10}Be/^{9}Be). This hypothesized lowering of riverine ^{10}Be/^{9}Be ratios due to small rivers would require a stronger atmospheric source for all basins, including the Northern and Central basins.

Based on measured ^{10}Be fluxes into sediment cores and estimated riverine (sedimentary) ^{10}Be fluxes, Aldahan et al. (1999) estimated that on the Buguldeika Saddle (between Southern and Central Basins), 35–40% of total ^{10}Be fluxes are derived from atmospheric inputs, in good agreement with our estimate for the Southern Basin. This estimate is slightly lower than GCM-based atmospheric ^{10}Be flux estimates (Heikkilä and Smith, 2013; Heikkilä et al., 2013; Heikkilä and von Blanckenburg, 2015). Of the ~ 11 mmol ^{10}Be yr^{-1} deposited into the river catchments analyzed here, we detect 3.5% in the riverine dissolved load. The remaining 96.5 % is adsorbed to suspended particles, assuming steady state between deposition and riverine export. Comparing direct GCM derived atmospheric input into the lake with riverine delivery suggests that ~ 55% of ^{10}Be derives from the atmosphere directly and ~ 45% from riverine inputs (assuming that riverine ^{10}Be removal is equal to ^{9}Be removal and that atmosphere derived ^{10}Be in the lake partitions between dissolved and reactive phases like in the rivers).

Taken together, these results confirm that at Lake Baikal, in contrast to oceanic settings (von Blanckenburg and Bouchez, 2014), rivers are important ^{10}Be sources – both for reactive (Aldahan et al., 1999) and dissolved fluxes.

5. SUMMARY AND CONCLUSIONS

We have presented a detailed analysis of weathering processes in the watershed of Lake Baikal, with the principal

objectives to assess (i) the extent to which the dissolved chemistry of the lake records these weathering processes and (ii) the degree to which sediment records potentially reflect secular changes in their operation. At Lake Baikal, chemical weathering rates appear to be correlated with runoff and slope, though there may also be a residual impact from previous glaciations. The largest riverine input to Lake Baikal, the Selenga derives 42 mol% of cation fluxes from silicate weathering. Total denudation rates, deduced from meteoric $^{10}Be/^{9}Be$, are low in all catchments compared to the global average, and negatively correlated with chemical weathering rates. This counter-intuitive finding may result from the stabilizing effect of permafrost in catchments at the northern end of the lake. Much higher erosion rates implied in observed $^{10}Be/^{9}Be$ ratios, in comparison to those estimated from suspended river loads, highlight the importance of sediment storage within the Selenga river system. Preliminary data suggest that this may also be true for the Turka. While most of the riverine dissolved major element flux is transferred into the lake, many trace elements are removed and have much lower concentrations in the lake than in the rivers. We suggest, based on REE patterns, Ce*, and Mn, Fe-depth profiles in the lake, that this removal is the result of pH induced changes in dissolved-adsorbed partitioning at the river-lake interface, and the incorporation of trace elements into authigenic Fe-Mn (oxyhydr)oxide phases forming in the lake.

The Sr isotope composition of Lake Baikal is uniform and closely reflects that of the riverine inputs, suggesting that a robust sedimentary record of past lake chemistry would faithfully integrate weathering processes and rates in the catchment. Crucially for future studies of the response of the chemistry of the lake to environmentally-forced changes in catchment weathering, and in strong contrast to the oceans, the residence time of Sr in the lake is short (~330 years). More care will be required with records of Nd and Be because these elements have residence times that are much shorter than the residence time of water in the lake and are not well-mixed. On the other hand, this provides the opportunity to use records from multiple cores to extract more granular information on weathering processes, specific to sub-catchments, with their own local environmental drivers.

Because sedimentary archives at Lake Baikal cover at least the last 12 Myr (e.g. Kashiwaya et al., 2001; Williams et al., 2001), the site has tremendous potential for studying the evolution of chemical weathering rates in the past, including during the Quaternary glacial cycles. Based on increasing LREE depletion (decreasing $(La/Yb)_n$), decreasing Fe and Mn concentrations, and accentuated Ce anomalies with depth, we have demonstrated that authigenic Fe-Mn oxyhydroxide phases are forming in the lake. This identification of the same removal process that occurs in the ocean suggests a way forward in terms of building such records. Potential difficulty will be in distinguishing the integrated record that would come from such phases formed in the lake, versus those that were flushed into the lake from terrestrial soils.

Overall, given the careful construction of sedimentary records using suitable core locations and adequate methods of extraction, this study highlights the potential for large lake systems to better constrain the relationship between environmental forcing factors and weathering, while also sampling significant areas of the continents such that the information has global implications.

Declaration of Competing Interest

The authors declare that they have no known competing financial interests or personal relationships that could have appeared to influence the work reported in this paper.

ACKNOWLEDGEMENTS

We would like to thank M. Sturm for initiating the research collaboration between ETH and the Siberian Branch of the RAS, G. de Souza and T.V. Popova for their help during the sampling campaign, N. Brinkmann, H. Gies, Q. Charbonnier, and M. Lupker for their help with the inverse model, R. Kissner for measuring the anion samples, and M. Lagarde for her help with the REE measurements. We further thank E. Tipper, F. von Blanckenburg, and an anonymous reviewer for their constructive reviews. This research was supported by ETH Zürich (Grant ETH-01 17-1).

APPENDIX A. SUPPLEMENTARY DATA

Research Data associated with this article is included in the electronic appendix (supplement S4). Supplementary data to this article can be found online at https://doi.org/10.1016/j.gca.2022.01.007.

REFERENCES

Abbott A. N., Haley B. A., McManus J. and Reimers C. E. (2015) The sedimentary flux of dissolved rare earth elements to the ocean. *Geochim. Cosmochim. Acta* **154**, 186–200.

Afanasjev A. N. (1976) *The water resources and water balance of Lake Baikal basin*. Nauk, Novosib, [in Russian].

Agafonov B. P. (1990) *Exolithodynamics of the Baikal rift zone*. Nauk, Novosib, [in Russian].

Ahnert F. (1970) Functional relationships between denudation, relief, and uplift in large, mid-latitude drainage basins. *Am. J. Sci.* **268**, 243–263.

Aldahan A., Possnert G., Peck J., King J. and Colman S. (1999) Linking the 10Be continental record of Lake Baikal to marine and ice archives of the last 50 ka : Implication for the global dust-aerosol input. *Geophys. Res. Lett.* **26**, 2885–2888.

Ambrosetti W., Barbanti L. and Sala N. (2003) Residence time and physical processes in lakes. *J. Limnol.* **62**, 1–15.

Anokhin Y. A., Ostromogilskii A. N. and Kokorin A. 0. (1991) Total balance of chemical substances in Lake Baikal [in Russian]. In *Monitoring of Lake Baikal environment* Hydrometeoizdat, Leningrad. pp. 153–158

Bagard M. L., Chabaux F., Pokrovsky O. S., Viers J., Prokushkin A. S., Stille P., Rihs S., Schmitt A. D. and Dupré B. (2011) Seasonal variability of element fluxes in two Central Siberian rivers draining high latitude permafrost dominated areas. *Geochim. Cosmochim. Acta* **75**, 3335–3357.

Bagard M. L., Schmitt A. D., Chabaux F., Pokrovsky O. S., Viers J., Stille P., Labolle F. and Prokushkin A. S. (2013) Biogeochemistry of stable Ca and radiogenic Sr isotopes in a larch-covered permafrost-dominated watershed of Central Siberia. *Geochim. Cosmochim. Acta* **114**, 169–187.

Bau M. (1999) Scavenging of dissolved yttrium and rare earths by precipitating iron oxyhydroxide: Experimental evidence for Ce oxidation, Y-Ho fractionation, and lanthanide tetrad effect. *Geochim. Cosmochim. Acta* **63**, 67–77.

Berner E. K. and Berner R. A. (2012) *Global environment: water, air, and geochemical cycles*. Princeton University Press.

Bertram C. J. and Elderfield H. (1993) The geochemical balance of the rare earth elements and neodymium isotopes in the oceans. *Geochim. Cosmochim. Acta* **57**, 1957–1986.

Biller D. V. and Bruland K. W. (2012) Analysis of Mn, Fe Co, Ni, Cu, Zn, Cd, and Pb in seawater using the Nobias-chelate PA1 resin and magnetic sector inductively coupled plasma mass spectrometry (ICP-MS). *Mar. Chem.* **130–131**, 12–20.

von Blanckenburg F. (2005) The control mechanisms of erosion and weathering at basin scale from cosmogenic nuclides in river sediment. *Earth Planet. Sci. Lett.* **237**, 462–479.

von Blanckenburg F. and Bouchez J. (2014) River fluxes to the sea from the ocean's 10Be/9Be ratio. *Earth Planet. Sci. Lett.* **387**, 34–43.

von Blanckenburg F., Bouchez J. and Wittmann H. (2012) Earth surface erosion and weathering from the 10Be (meteoric)/ 9Be ratio. *Earth Planet. Sci. Lett.* **351–352**, 295–305.

Blum J. D. and Erel Y. (2003) Radiogenic isotopes in weathering and hydrology. *Treatise Geochem.* **5–9**, 365–392.

Boyle E. A., Edmond J. M. and Sholkovitz E. R. (1977) The mechanism of iron removal in estuaries. *Geochim. Cosmochim. Acta* **41**, 1313–1324.

Boyle E., Collier R. and Dengler A. T. (1974) On the chemical mass-balance in estuaries. *Geochim. Cosmochim. Acta* **38**, 1719–1728.

Brantley S. L. (2003) Reaction kinetics of primary rock-forming minerals under ambient conditions. *Treatise on Geochemistry* **5**, 73–117.

Bring A., Fedorova I., Dibike Y., Hinzman L., Mård J., Mernild S. H., Prowse T., Semenova O., Stuefer S. L. and Woo M. K. (2016) Arctic terrestrial hydrology: A synthesis of processes, regional effects, and research challenges. *J. Geophys. Res. Biogeosci.* **121**, 621–649.

Bufe A., Hovius N., Emberson R., Rugenstein J. K. C., Galy A., Hassenruck-gudipati H. J. and Chang J. (2021) Co-variation of silicate, carbonate and sulfide weathering drives CO2 release with erosion. *Nat. Geosci.*, 14.

Chalov S. R., Jarsjö J., Kasimov N. S. O., Romanchenko A., Pietroń J., Thorslund J. and Promakhova E. V. (2014) Spatio-temporal variation of sediment transport in the Selenga River Basin, Mongolia and Russia. *Environ. Earth Sci.* **73**, 663–680.

Christl M., Vockenhuber C., Kubik P. W., Wacker L., Lachner J., Alfimov V. and Synal H. A. (2013) The ETH Zurich AMS facilities: Performance parameters and reference materials. *Nucl. Instrum. Methods Phys. Res. Sect. B Beam Interact. Mater. Atoms* **294**, 29–38.

Colman S. M. (1998) Water-level changes in Lake Baikal, Siberia: tectonism versus climate. *Geology* **26**, 531–534.

Colombo N., Salerno F., Gruber S., Freppaz M., Williams M., Fratianni S. and Giardino M. (2018) Review: Impacts of permafrost degradation on inorganic chemistry of surface fresh water. *Glob. Planet. Change* **162**, 69–83.

Deberdt S., Viers J. and Dupré B. (2002) New insights about the rare earth elements (REE) mobility in river waters. *Bull. la Société Géologique Fr.* **173**, 147–160.

Dellinger M., Gaillardet J., Bouchez J., Calmels D., Louvat P., Dosseto A., Gorge C., Alanoca L. and Maurice L. (2015) Riverine Li isotope fractionation in the Amazon River basin controlled by the weathering regimes. *Geochim. Cosmochim. Acta* **164**, 71–93.

Deniel C. and Pin C. (2001) Single-stage method for the simultaneous isolation of lead and strontium from silicate samples for isotopic measurements. *Anal. Chim. Acta* **426**, 95–103.

Drever J. I. (1998) *The Geochemistry of Natural Waters: Surface and Groundwater Environments*, third ed. Prentice Hall, Englewood Cliffs.

Fagel N., Thamó-Bózsó E. and Heim B. (2007) Mineralogical signatures of Lake Baikal sediments: Sources of sediment supplies through Late Quaternary. *Sediment. Geol.* **194**, 37–59.

Falkner K., Church M., LeBaron G., Thouron D., Jeandel C., Stordal M., Gill G., Mortlock R., Froelich P. and Chan L. (1997) Minor and trace element chemistry of Lake Baikal, its tributaries, and surrounding hot springs Available at:. *Limnol. Oceanogr.* **42**, 329–345 http://scholarsarchive.library.oregonstate.edu/jspui/handle/1957/12855.

Falkner K. K., Measures C. I., Herbelin S. E., Edmond J. A. and Weiss R. F. (1991) The major and minor element geochemistry of Lake Baikal. *Limnol. Oceanogr.* **36**, 413–423.

Fitzsimons M. F., Lohan M. C., Tappin A. D. and Millward G. E. (2012) *The Role of Suspended Particles in Estuarine and Coastal Biogeochemistry*. Elsevier Inc..

Foster G. L. and Vance D. (2006) In situ Nd isotopic analysis of geological materials by laser ablation MC-ICP-MS. *J. Anal. At. Spectrom.* **21**, 288–296.

Frey K. E. and McClelland J. W. (2009) Impacts of permafrost degradation on arctic river biogeochemistry Available at:. *Hydrol. Process.* **23**, 169–182 http://jamsb.austms.org.au/courses/CSC2408/semester3/resources/ldp/abs-guide.pdf.

Frey K. E., Siegel D. I. and Smith L. C. (2007) Geochemistry of west Siberian streams and their potential response to permafrost degradation. *Water Resour. Res.* **43**.

Gaillardet J., Dupré B., Allègre C. J. and Négrel P. (1997) Chemical and physical denudation in the Amazon River Basin. *Chem. Geol.* **142**, 141–173.

Gaillardet J., Dupré B., Louvat P. and Allègre C. J. (1999) Global silicate weathering and CO2 consumption rates deduced from the chemistry of large rivers. *Chem. Geol.* **159**, 3–30.

Galazy G. I. (1993) Atlas ozera Baikal. *Russ. Geod. Map Serv. Moscow*, [in Russian].

Gislason S. R., Oelkers E. H., Eiriksdottir E. S., Kardjilov M. I., Gisladottir G., Sigfusson B., Snorrason A., Elefsen S., Hardardottir J., Torssander P. and Oskarsson N. (2009) Direct evidence of the feedback between climate and weathering. *Earth Planet. Sci. Lett.* **277**, 213–222.

Gladkochub D. P., Donskaya T. V., Reddy S. M., Poller U., Bayanova T. B., Mazukabzov A. M., Dril S., Todt W. and Pisarevsky S. A. (2009) Palaeoproterozoic to Eoarchaean crustal growth in southern Siberia: A Nd-isotope synthesis. *Geol. Soc. Spec. Publ.* **323**, 127–143.

Goldberg E. L., Chebykin E. P., Zhuchenko N. A., Vorobyeva S. S., Stepanova O. G., Khlystov O. M., Ivanov E. V., Weinberg E. and Gvozdkov A. N. (2010) Uranium isotopes as proxies of the environmental history of the Lake Baikal watershed (East Siberia) during the past 150ka. *Palaeogeogr. Palaeoclimatol. Palaeoecol.* **294**, 16–29.

Goldstein S. J. and Jacobsen S. B. (1987) The Nd and Sr isotopic systematics of river-water dissolved material Implications for the sources of Nd and Sr in seawater. *Chem. Geol.* **66**, 245–272. Available at: file:///Users/rventura/Dropbox/robertoventura's library/Library.papers3/files/Goldstein 1987 The Nd and Sr isotopic systematics of river-water dissolved material Implications for the sources of Nd and Sr in seawater.pdf%0Apapers3://publication/uuid/D29CF3.

Granina L. (1997) The chemical budget of Lake Baikal: A review Available at:. *Limnol. Oceanogr.* **42**, 373–378 http://www.jstor.org/stable/10.2307/2838565.

Gustafsson Ö. and Gschwend P. M. (1997) Aquatic colloids: Concepts, definitions, and current challenges. *Limnol. Oceanogr.* **42**, 519–528.

Hartmann J. (2009) Bicarbonate-fluxes and CO2-consumption by chemical weathering on the Japanese Archipelago — Application of a multi-lithological model framework. *Chem. Geol.* **265**, 237–271.

Hartmann J., Moosdorf N., Lauerwald R., Hinderer M. and West A. J. (2014) Global chemical weathering and associated p-release - the role of lithology, temperature and soil properties. *Chem. Geol.* **363**, 145–163.

Hatje V., Bruland K. W. and Flegal A. R. (2014) Determination of rare earth elements after pre-concentration using NOBIAS-chelate PA-1®resin: Method development and application in the San Francisco Bay plume. *Mar. Chem.* **160**, 34–41.

Heikkilä U., Beer J., Abreu J. A. and Steinhilber F. (2013) On the atmospheric transport and deposition of the cosmogenic radionuclides (10Be): A review. *Space Sci. Rev.* **176**, 321–332.

Heikkilä U. and von Blanckenburg F. (2015) The global distribution of Holocene meteoric 10Be fluxes from atmospheric models. Distribution maps for terrestrial Earth surface applications.

Heikkilä U. and Smith A. M. (2013) Production rate and climate influences on the variability of 10Be deposition simulated by ECHAM5-HAM: Globally, in Greenland, and in Antarctica. *J. Geophys. Res. Atmos.* **118**, 2506–2520.

Heim, B., Klump, J., Schulze, A., Schneider, S., Swiercz, S., Dachnowski, G., Fagel N. (2007) Lithological map of the Lake Baikal catchment.

Hindshaw R. S., Teisserenc R., Le Dantec T. and Tananaev N. (2019) Seasonal change of geochemical sources and processes in the Yenisei River: A Sr, Mg and Li isotope study. *Geochim. Cosmochim. Acta* **255**, 222–236.

Hohmann R., Kipfer R., Peeters F., Piepke G., Imboden D. M. and Shimaraev M. N. (1997) Processes of deep-water renewal in Lake Baikal Available at:. *Limnol. Oceanogr.* **42**, 841–855 http://www.aslo.org/lo/toc/vol_42/issue_5/0841.html.

Hus R., De Batist M., Klerkx J. and Matton C. (2006) Fault linkage in continental rifts: structure and evolution of a large relay ramp in Zavarotny; Lake Baikal (Russia). *J. Struct. Geol.* **28**, 1338–1351.

Imran U., Weidhaas J., Ullah A. and Shaikh K. (2021) Risk associated with spatio-temporal variations in trace metals and a metalloid in a major freshwater reservoir of Pakistan. *Hum. Ecol. Risk Assess.* **27**, 431–450.

Jeandel C., Peucker-Ehrenbrink B., Jones M. T., Pearce C. R., Oelkers E. H., Godderis Y., Lacan F., Aumont O. and Arsouze T. (2011) Ocean margins: The missing term in oceanic element budgets? *EOS Trans. Am. Geophys. Union* **92**, 217–224.

Karabanov E. B., Prokopenko A. A., Williams D. F. and Colman S. M. (1998) Evidence from Lake Baikal for Siberian glaciation during oxygen-isotope substage 5d. *Quat. Res.* **50**, 46–55.

Karabanov E., Williams D., Kuzmin M., Sideleva V., Khursevich G., Prokopenko A., Solotchina E., Tkachenko L., Fedenya S., Kerber E., Gvozdkov A., Khlustov O., Bezrukova E., Letunova P. and Krapivina S. (2004) Ecological collapse of Lake Baikal and Lake Hovsgol ecosystems during the Last Glacial and consequences for aquatic species diversity. *Palaeogeogr. Palaeoclimatol. Palaeoecol.* **209**, 227–243.

Kashiwaya K., Ochiai S., Sakai H. and Kawai T. (2001) Orbit-related long-term climate cycles revealed in a 12-Myr continental record Lake Baikal. *Nature* **410**, 71–74.

Killworth P. D., Carmack E. C., Weiss R. F. and Matear R. (1996) Modeling deep-water renewal in Lake Baikal. *Limnol. Oceanogr.* **41**, 1521–1538.

Kipfer R., Aeschbach-Hertig W., Hopfer M., Hohmann R., Imboden D. M., Baur H., Golubev V. and Klerkx J. (1996) Bottomwater formation due to hydrothermal activity in Frolikha Bay, Lake Baikal, eastern Siberia. *Geochem. Cosmochem. Acta* **6**, 961–971.

Kirchner J. W., Finkel R. C., Riebe C. S., Granger D. E., Clayton J. L., King J. G. and Megahan W. F. (2001) Mountain erosion over 10 yr, 10 k.y., and 10 m.y. time scales. *Geology* **29**, 591–594.

Kulish E. A. (1983) Sedimentary geology of the Archaean of the aldan schield. *Nauk. Moscow*, 206, [in Russian].

Lacan F. and Jeandel C. (2005) Neodymium isotopes as a new tool for quantifying exchange fluxes at the continent-ocean interface. *Earth Planet. Sci. Lett.* **232**, 245–257.

Larsen I. J., Montgomery D. R. and Greenberg H. M. (2014) The contribution of mountains to global denudation. *Geology* **42**, 527–530.

Leibovich-Granina L. Z. (1987) Iron and manganese cycle in Lake Baikal. *Vodn. Resur.* **15**, 67–72.

MacLean R., Oswood M. W., Irons J. G. and Mcdowell W. H. (1999) The effect of permafrost on stream biogeochemistry: A case study of two streams in the Alaskan (U.S.A.) taiga. *Biogeochemistry* **47**, 239–267.

Martin P., Granina L., Martens K. and Goddeeris B. (1998) Oxygen concentration profiles in sediments of two ancient lakes: Lake Baikal (Siberia, Russia) and Lake Malawi (East Africa). *Hydrobiologia* **367**, 163–174.

Mats V. D. (1993) The structure and development of the Baikal rift depression. *Earth Sci. Rev.* **34**, 81–118.

Matton C. and Klerkx J. (1995) Basin structure in the western part of Northern Lake Baikal: the Zavorotny area. *Russ. Geol. Geophys. C/C Geol. I Geofiz.* **36**, 168–174.

McClelland J. W., Holmes R. M., Peterson B. J., Raymond P. A., Striegl R. G., Zhulidov A. V., Zimov S. A., Zimov N., Tank S. E., Spencer R. G. M., Staples R., Gurtovaya T. Y. and Griffi C. G. (2016) Particulate organic carbon and nitrogen export from major Arctic rivers. *Global Biogeochem. Cycles* **30**, 629–643.

Meybeck M. (2003) Global Occurence of Major Elements in Rivers. In *Treatise on Geochemistry* p. 207.223.

Michard A., Albarède F., Michard G., Minster J. F. and Charlou J. L. (1983) Rare-earth elements and uranium in high-temperature solutions from east pacific rise hydrothermal vent field (13 °N). *Nature* **303**, 795–797.

Milliman J. D. and Farnsworth K. L. (2013) *River Discharge to the Coastal Ocean: A Global Synthesis*. Cambridge University Press.

Moffett J. W. (1994) The relationship between cerium and manganese oxidation in the marine environment. *Limnol. Oceanogr.* **39**, 1309–1318.

Montgomery D. R. and Brandon M. T. (2002) Topographic controls on erosion rates in tectonically active mountain ranges. *Earth Planet. Sci. Lett.* **201**, 481–489.

Müller A. M., Christl M., Lachner J., Suter M. and Synal H. A. (2010) Competitive 10Be measurements below 1 MeV with the upgraded ETH-TANDY AMS facility. *Nucl. Instrum. Methods Phys. Res. Sect. B Beam Interact. Mater. Atoms* **268**, 2801–2807.

Négrel P., Allègre C. J., Dupré B. and Lewin E. (1993) Erosion sources determined by inversion of major and trace element ratios and strontium isotopic ratios in river: The Congo Basin case. *Earth Planet. Sci. Lett.* **120**, 59–76.

Olivarez L. A. and Lyle M. W. (2002) Determination of biogenic silica in pelagic marine sediments: a simple method revisted. *Proc. ODP, Initial Reports* **199**, 1–21.

Ouimet W. B., Whipple K. X. and Granger D. E. (2009) Beyond threshold hillslopes: Channel adjustment to base-level fall in tectonically active mountain ranges. *Geology* **37**, 579–582.

Parfenov L. M., Khanchuk A. I., Badarch G., Miller R. J., Naumova V. V., Nokleberg W. J., Ogasawara M., Prokopiev A. V. and Yan H. (2003) Preliminary northeast Asia geodynamics map. *US Geological Survey*.

Peeters F., Kipfer R., Hohmann R., Hofer M., Imboden D. M., Kodenev G. G. and Khozder T. (1997) Modeling transport rates in lake baikal: gas exchange and deep water renewal. *Environ. Sci. Technol.* **31**, 2973–2982.

Petrov O. V., Leonov Y. G., Tingdong L. and Tomurtogoo O. (2007) Tectonic map of Northern-Central-Eastern Asia and adjacent areas, 192.

Pham V. Q., Grenier M., Cravatte S., Michael S., Jacquet S., Belhadj M., Nachez Y., Germineaud C. and Jeandel C. (2019) Dissolved rare earth elements distribution in the Solomon Sea. *Chem. Geol.* **524**, 11–36.

Pin C. and Zalduegui J. F. S. (1997) Sequential separation of light rare-earth elements, thorium and uranium by miniaturized extraction chromatography: Application to isotopic analyses of silicate rocks. *Analytica Chim. Acta* **339**, 79–89.

Potemkina T. G. (2011) Sediment runoff formation trends of major tributaries of Lake Baikal in the 20th century and at the beginning of the 21st century. *Russ. Meteorol. Hydrol.* **36**, 819–825.

Poulton S. W. and Raiswell R. (2002) The low-temperature geochemical cycle of iron: from continental fluxes to marine sediment deposition. *Am. J. Sci.* **302**, 774–805.

Prokushkin A. S., Gleixner G., McDowell W. H., Ruehlow S. and Schulze E. D. (2007) Source- and substrate-specific export of dissolved organic matter from permafrost-dominated forested watershed in central Siberia. *Global Biogeochem. Cycles* **21**, 1–12.

Rahaman W., Wittmann H. and von Blanckenburg F. (2017) Denudation rates and the degree of chemical weathering in the Ganga River basin from ratios of meteoric cosmogenic 10Be to stable 9Be. *Earth Planet. Sci. Lett.* **469**, 156–169.

Rempfer J., Stocker T. F., Joos F., Dutay J. C. and Siddall M. (2011) Modelling Nd-isotopes with a coarse resolution ocean circulation model: Sensitivities to model parameters and source/sink distributions. *Geochim. Cosmochim. Acta* **75**, 5927–5950.

Rickli J., Frank M., Stichel T., Georg R. B., Vance D. and Halliday A. N. (2013) Controls on the incongruent release of hafnium during weathering of metamorphic and sedimentary catchments. *Geochim. Cosmochim. Acta* **101**, 263–284.

Rickli J., Hindshaw R. S., Leuthold J., Wadham J. L., Burton K. W. and Vance D. (2017) Impact of glacial activity on the weathering of Hf isotopes – Observations from Southwest Greenland. *Geochim. Cosmochim. Acta* **215**, 295–316.

Rousseau T. C. C., Sonke J. E., Chmeleff J., Van Beek P., Souhaut M., Boaventura G., Seyler P. and Jeandel C. (2015) Rapid neodymium release to marine waters from lithogenic sediments in the Amazon estuary. *Nat. Commun.*, 6.

Schaller M., von Blanckenburg F., Hovius N. and Kubik P. W. (2001) Large-scale erosion rates from in situ-produced cosmogenic nuclides in European river sediments. *Earth Planet. Sci. Lett.* **188**, 441–458.

Schijf J., Christenson E. A. and Byrne R. H. (2015) YREE scavenging in seawater: A new look at an old model. *Mar. Chem.* **177**, 460–471.

Schindler P. W. and Stumm W. (1987) The surface chemistry of oxides, hydroxides, and oxide minerals. *Aquat. Surf. Chem. Chem. Process. Part. Interface. John Wiley Sons, New York* **1987**, 83–110, 13 fig, 7 tab, 49 ref.

Seal R. R. and Shanks W. C. (1998) Oxygen and hydrogen isotope systematics of Lake Baikal, Siberia: Implications for paleoclimate studies. *Limnol. Oceanogr.* **43**, 1251–1261.

Shanks W. C. and Callender E. (1992) Thermal springs in Lake Baikal. *Geology* **20**, 495–497.

Sherstyankin P. P., Alekseev S. P., Abramov A. M., Stavrov K. G., Batist M., Hus R., Canals M. and Casamor J. L. (2006) Computer-based bathymetric map of Lake Baikal. *Dokl. Earth Sci.* **408**, 564–569.

Shimaraev M. N. (1994) Physical limnology of Lake Baikal: A review. *Phys. Limnol. Lake Baikal a Rev.*

Shimaraev M. N., Granin N. G. and Zhdanov A. A. (1993) Deep ventilation of Lake Baikal waters due to spring thermal bars. *Limnol. Oceanogr.* **38**, 1068–1072.

Sholkovitz E. R. (1995) The aquatic chemistry of rare earth elements in rivers and estuaries. *Aquat. Geochemistry* **1**, 1–34.

Sholkovitz E. R. (1978) The flocculation of dissolved Fe, Mn, Al, Cu, Ni, Co and Cd during estuarine mixing. *Earth Planet. Sci. Lett.* **41**, 77–86.

Sklyarova O. A., Sklyarov E. V., Och L., Pastukhov M. V. and Zagorulko N. A. (2017) Rare earth elements in tributaries of Lake Baikal (Siberia, Russia). *Appl. Geochem.* **82**, 164–176.

Stichel T., Pahnke K., Duggan B., Goldstein S. L., Hartman A. E., Paffrath R. and Scher H. D. (2018) TAG plume: Revisiting the hydrothermal neodymium contribution to seawater. *Front. Mar. Sci.*, 5.

Suhrhoff T. J., Rickli J., Crocket K., Nakic E. B. and Vance D. (2019) Behavior of beryllium in the weathering environment and its delivery to the ocean. *Geochem. Cosmochem. Acta* **265**, 1–44.

Tarasova E. N. and Mescheryakova A. I. (1992) Modern state of hydrochemical regime of Lake Baikal. *Nauk Novosib*, [in Russian].

Taylor S. R. and McLennan S. M. (1985) *The continental crust: its composition and evolution*. Blackwell Scientific Pub, Palo Alto, CA.

Temnerud J., Düker A., Karlsson S., Allard B., Bishop K., Fölster J. and Köhler S. (2013) Spatial patterns of some trace elements in four Swedish stream networks. *Biogeosciences* **10**, 1407–1423.

Thirlwall M. F. (1991) Long-term reproducibility of multicollector Sr and Nd isotope ratio analysis. *Chem. Geol.* **94**, 85–104.

Tipper E. T., Bickle M. J., Galy A., West A. J., Pomiès C. and Chapman H. J. (2006) The short term climatic sensitivity of carbonate and silicate weathering fluxes: Insight from seasonal variations in river chemistry. *Geochim. Cosmochim. Acta* **70**, 2737–2754.

Tulokhonov A. K., Plyusnin V. M., Kudelya S. V. and Beshentsev A. N. (2015) *The Ecological Atlas of the Baikal Basin*., Institute of geography V.B. Sochava SB RAS.

Vance D., Little S. H., Archer C., Cameron V., Andersen M. B., Rijkenberg M. J. A. and Lyons T. W. (2016) The oceanic budgets of nickel and zinc isotopes: The importance of sulfdic environments as illustrated by the Black Sea. *Philos. Trans. R. Soc. A Math. Phys. Eng Sci*, 374.

Vance D. and Thirlwall M. (2002) An assessment of mass discrimination in MC-ICPMS using Nd isotopes. *Chem. Geol.* **185**, 227–240.

Viers J., Oliva P., Dandurand J. L., Dupré B. and Gaillardet J. (2013) Chemical weathering rates, CO2 consumption, and control parameters deduced from the chemical composition of rivers. *Treatise Geochem. Second Ed.* **7**, 175–194.

Walvoord M. A., Voss C. I. and Wellman T. P. (2012) Influence of permafrost distribution on groundwater flow in the context of climate-driven permafrost thaw: Example from Yukon Flats Basin, Alaska, United States. *Water Resour. Res.* **48**, 1–17.

Weiss R. F., Carmack E. C. and Koropalov V. M. (1991) Deep-water renewal and biological production in Lake Baikal. *Nature* **349**, 665–669.

White A. F. and Blum A. E. (1995) Effects of climate on chemical weathering in watersheds. *Geochim. Cosmochim. Acta* **59**, 1729–1747.

Wiederhold J. G., Teutsch N., Kraemer S. M., Halliday A. N. and Kretzschmar R. (2007) Iron isotope fractionation in oxic soils by mineral weathering and podzolization. *Geochim. Cosmochim. Acta* **71**, 5821–5833.

Willenbring J. K. and von Blanckenburg F. (2010) Meteoric cosmogenic Beryllium-10 adsorbed to river sediment and soil: Applications for Earth-surface dynamics. *Earth-Sci. Rev.* **98**, 105–122.

Williams D. F., Kuzmin M. I., Prokopenko A. A., Karabanov E. B., Khursevich G. K. and Bezrukova E. V. (2001) The Lake Baikal drilling project in the context of a global lake drilling initiative. *Quat. Int.* **80–81**, 3–18.

Williams P. J. and Warren I. M. T. (1999) The English Language Edition of the Geocryological Map of Russia and Neighbouring Republics: A Project of Moscow State University, Department of Geocryology, Cambridge University, Scott Polar Research Institute, and Carleton University, Geotechnical Scien. *Collaborative Map Project*.

Wittmann H., von Blanckenburg F., Dannhaus N., Bouchez J., Gaillardet J., Guyot J. L., Maurice L., Roig H., Filizola N. and Christl M. (2015) A test of the cosmogenic 10Be(meteoric)/9Be proxy for simultaneously determining basin-wide erosion rates, denudation rates, and the degree of weathering in the Amazon basin. *J. Geophys. Res. Earth Surf.* **119**, 2448–2459.

Wittmann H., Oelze M., Gaillardet J., Garzanti E. and von Blanckenburg F. (2020) A global rate of denudation from cosmogenic nuclides in the Earth's largest rivers Available at:. *Earth-Sci. Rev.* **204** https://linkinghub.elsevier.com/retrieve/pii/S0012825219304039 103147.

Wittmann H., Oelze M., Roig H. and von Blanckenburg F. (2018) Are seasonal variations in river-floodplain sediment exchange in the lower Amazon River basin resolvable through meteoric cosmogenic 10Be to stable 9Be ratios? *Geomorphology* **322**, 148–158.

Yanshin A. L. (1989) Ekzogennoe porodo- and rudo-obrazo- vanie v dokembrii. *Nauk. Moscow*, 206, [in Russian].

Yeghicheyan D., Aubert D., Bouhnik-Le C. M., Chmeleff J., Delpoux S., Djouraev I., Granier G., Lacan F., Piro J. L., Rousseau T., Cloquet C., Marquet A., Menniti C., Pradoux C., Freydier R., Vieira da Silva-Filho E. and Suchorski K. (2019) A new interlaboratory characterisation of silicon, rare earth elements and twenty-two other trace element concentrations in the natural river water certified reference material SLRS-6 (NRC-CNRC). *Geostand. Geoanal. Res.* **43**, 475–496.

Yokoo Y., Nakano T., Nishikawa M. and Quan H. (2004) Mineralogical variation of Sr-Nd isotopic and elemental compositions in loess and desert sand from the central Loess Plateau in China as a provenance tracer of wet and dry deposition in the northwestern Pacific. *Chem. Geol.* **204**, 45–62.

Yoshioka T., Ueda S., Khodzher T., Bashenkhaeva N., Korovyakova I., Sorokovikova L. and Gorbunova L. (2002) Distribution of dissolved organic carbon in Lake Baikal and its watershed Available at:. *Limnology* **3**, 159–168 http://link.springer.com/10.1007/s102010200019.

You C.-F., Lee T. and Li Y.-H. (1989) The partition of Be between soil and water. *Chem. Geol.* **77**, 105–118.

Zakharova E. A., Pokrovsky O. S., Dupré B. and Zaslavskaya M. B. (2005) Chemical weathering of silicate rocks in Aldan Shield and Baikal Uplift: Insights from long-term seasonal measurements of solute fluxes in rivers. *Chem. Geol.* **214**, 223–248.

Associate editor: Nathalie Vigier